

**The University of South Bohemia in České Budějovice
Faculty of Science**

Immunometabolic Tumor Therapy
Bachelor's thesis

Benjamin Schatzmann

Supervisor: Mgr. Radka Lencová
Co-supervisor: RNDr. Jan Ženka, CSc.

České Budějovice 2023

**Schatzmann, B., 2023: Immunometabolic Tumor Therapy. Bc. Thesis, in English. – 59 p.,
Faculty of Science, University of South Bohemia, České Budějovice, Czech Republic.**

Annotation

MBTA therapy (mixture of mannan-BAM, Toll-like receptor agonists and anti-CD40 antibody) is a cancer immunotherapy developed by Dr. Ženka. This thesis investigates options of MBTA therapy in combination with the glutamine metabolism inhibitor 6-diazo-5-oxo-L-norleucine (DON). The dosage of DON, ways of application, and side effects on mice were investigated. Also, the option of replacing the mannan-BAM with a more specified molecule was researched.

Keywords: Immunotherapy, Cancer, MBTA, DON, fMLF

I declare that I am the author of this qualification thesis and that in writing it I have used the sources and literature displayed in the list of used sources only.

Linz, November 27, 2023

.....
Student's signature

Content

1. Introduction	1
1.1. Cancer.....	1
1.1.1. Incidence	1
1.1.2. Pancreatic Adenocarcinoma.....	1
1.1.3. Pancreatic Adenocarcinoma as a Laboratory Model.....	2
1.1.4. The Cancerous Phenotype.....	3
1.1.5. The Hallmarks of Cancer	3
1.1.6. Self-Sufficiency in Growth Signals.....	4
1.1.7. Insensitivity to Anti-Growth Signals.....	5
1.1.8. Evading Apoptosis.....	5
1.1.9. Limitless Replicative Potential.....	6
1.1.10. Sustained Angiogenesis	7
1.1.11. Tissue Invasion and Metastasis	7
1.1.12. Further Hallmarks.....	8
1.2. Glucose Metabolism and The Warburg Effect	8
1.2.1. Glutamine Addiction	9
1.3. Types of Cancer Therapy	11
1.4. Chemotherapy	11

1.4.1.	A History of Chemotherapy	11
1.4.2.	6-diazo-5-oxo-L-norleucine	12
1.5.	Immunotherapy	13
1.5.1.	Immunity.....	13
1.5.2.	Approaches in Immunotherapy	15
1.6.	MBTA Therapy.....	15
1.6.1.	Mannan-BAM	16
1.6.2.	TLR Agonists	17
1.6.3.	Anti-CD40 Antibody	18
1.6.4.	Limitations of MBTA and DON Therapies	19
1.7.	fMLF	20
2.	Aims	21
3.	Materials and Methods	22
3.1.	List of Chemicals	22
3.2.	Preparation of Chemicals.....	22
3.2.1.	Manan-BAM	22
3.2.2.	MBTA Mixture and its Modifications	23
3.2.3.	6-diazo-5-oxo-L-norleucine (DON)	24
3.2.4.	Mixture for Trypsinization of Cultivated Cells.....	24
3.3.	Mice.....	24
3.4.	Cell Line and Cultivation	25

3.4.1.	Preparation of Panc02 Cells for <i>In Vivo</i> Experiments	25
3.4.2.	Transplantation of Panc02 Cells.....	25
3.5.	Measurement of Tumors.....	26
3.5.1.	Calculation of Tumor Growth Reduction	26
3.5.2.	Calculation of the Area Under the Curve (AUC).....	26
3.5.3.	Statistical evaluation.....	27
3.6.	Schemas of Experiments	27
3.6.1.	Experiment I – DON Dose Escalation Study.....	27
3.6.2.	Experiment II – Optimization of DON Administration and Monitoring of Side Effects	28
3.6.3.	Experiment III – Exploring the Substitution of Mannan-BAM with fLMF .	30
4.	Results	31
4.1.	Experiment I	31
4.1.1.	Tumor volumes.....	31
4.1.2.	Survival.....	32
4.2.	Experiment II	32
4.2.1.	Tumor volumes.....	32
4.2.2.	Survival.....	35
4.2.3.	Food Consumption.....	40
4.2.4.	Water Consumption	41
4.3.	Experiment III.....	42

4.3.1. Mean Tumor Growth.....	42
4.3.2. Survival.....	44
5. Discussion	45
6. Conclusion.....	49
7. References	50

1. Introduction

This work is drawn up as part of Dr. Ženka's long-term research focused on the fight against cancer. Over the years, a therapeutic mixture that works as a tumor immunotherapy has been developed. Development of the therapeutics began by triggering the innate immunity against tumor cells, over time acquired immunity was involved, and currently, the team is working on combining therapeutical approaches to increase the therapeutic effect against tough tumor models (Ženka, Lencová, oral communication).

1.1. Cancer

1.1.1. Incidence

Cancer is one of the leading causes of death worldwide. Close to 10 million are estimated to have died of cancer in 2020, accounting for one in six deaths. The most common forms are breast cancer, lung cancer, and colorectal cancer. Lung cancer is the most fatal. Up to half of all cancers are thought to be preventable. Strategies include avoiding alcohol and tobacco, healthy diet and exercise, vaccination against HPV and hepatitis B, and avoiding radiation exposure. Outcomes can be improved by screening and early diagnosis (Sung et al., 2021; WHO, 2022).

Although Dr. Ženka's team works with several types of cancer, this work is focused only on the very difficult-to-treat model of pancreatic adenocarcinoma.

1.1.2. Pancreatic Adenocarcinoma

Pancreatic adenocarcinoma is the most common form of pancreatic cancer. It is associated with a poor prognosis. It has a low incidence compared to more common types of cancer but a

relatively high mortality rate. It is the fourth most common cause of cancer death (Siegel et al., 2023). The disease has already spread at diagnosis in 80% of cases (Vareedayah et al., 2018).

Smoking is among the most substantial risk factors for developing pancreatic adenocarcinoma. It has been associated with type 2 diabetes, but the underlying mechanism is unknown. There is a strong genetic component to the development of pancreatic cancer. Multiple genes increasing the probability of developing the disease have been identified. Susceptibility is hereditary, and afflicted relatives constitute a significant indication in risk assessment. Semiyearly screening is recommended for those at risk. A lack of early symptoms allows cancer to remain undetected for a long time in most cases. Treatments most commonly include surgery, chemotherapy, and radiotherapy (Vareedayah et al., 2018).

1.1.3. Pancreatic Adenocarcinoma as a Laboratory Model

In *in vivo* experiments, where the experiment aims to study cancer and its therapeutic approaches, it is necessary to induce tumor growth in the tested organism. This can be done in two ways: injecting a highly carcinogenic substance into the desired tissue or directly injecting the desired type of cancer cells into the organism. If mice are used as experimental subjects, it is necessary that this cell line also originates from a mouse of the same strain.

In this thesis, cells from the Panc02 line were used. This line was created by injecting 3-methyl-chloroanthrene into the pancreas of C57BL/6 mice and is characterized by its aggressive and undifferentiated growth pattern compared to other similar cell lines. Unfortunately, it lacks the mutational changes found in human adenocarcinoma, thus limiting its clinical relevance. However, it has wide application in laboratory studies (Partecke et al., 2011; Torres et al., 2013).

1.1.4. The Cancerous Phenotype

Cancer cells differ markedly from healthy ones. They exhibit aberrations in metabolism and altered gene expression, divide uncontrollably, and exploit mutations to evade intrinsic defense mechanisms. While every cancer is different, several common features are shared across various types of cancer. Distinguishing the signal transduction and metabolic pathways commonly affected by the disease is key to the development of treatments.

1.1.5. The Hallmarks of Cancer

In their 2000 review, Hanahan and Weinberg proposed a list of key characteristics of human cancer cells, which they termed the hallmarks of cancer. They outlined a conceptual framework consisting of six cellular-level capabilities acquired by cells that develop into tumor cells. They suggest that these traits are shared among most human cancers and enable premalignant cells to overcome the regulatory mechanisms that maintain homeostasis in healthy tissues. Virtually all hallmark capabilities are essential for a tumor to proliferate. Cancers differ in how they acquire the hallmark capabilities and the order in which they do so. The original hallmarks are self-sufficiency in growth signals, insensitivity to anti-growth signals, tissue invasion and metastasis, limitless replicative potential, sustained angiogenesis, and evading apoptosis. An emphasis was put on broadening our conception of tumors as complex tissue consisting of both aberrant and healthy cells exploited by cancer (Hanahan & Weinberg, 2000).

The authors later expanded on their theory, reviewing new insights into the hallmarks and going on to describe two additional emerging hallmarks, those being deregulating cellular metabolism and avoiding immune destruction, as well as two enabling characteristics, which are genome instability and tumor-promoting inflammation (Hanahan & Weinberg, 2011). Hanahan recently argued that the emerging hallmarks are indeed part of the core hallmarks of cancer, and they are now part of the model as seen in figure 1 (Hanahan, 2022).

The model has laid important groundwork for our understanding of cancer. Over the years, it has been met with criticism, accusing the authors of oversimplifying and adding that most hallmarks are also shared with benign growths. Alternative conceptions of the model have also been proposed (Fouad & Aanei, 2017).

Major hallmarks of interest, along with their underlying mechanisms, will be summarized below, with emphasis on major pathways rather than exhaustive coverage.

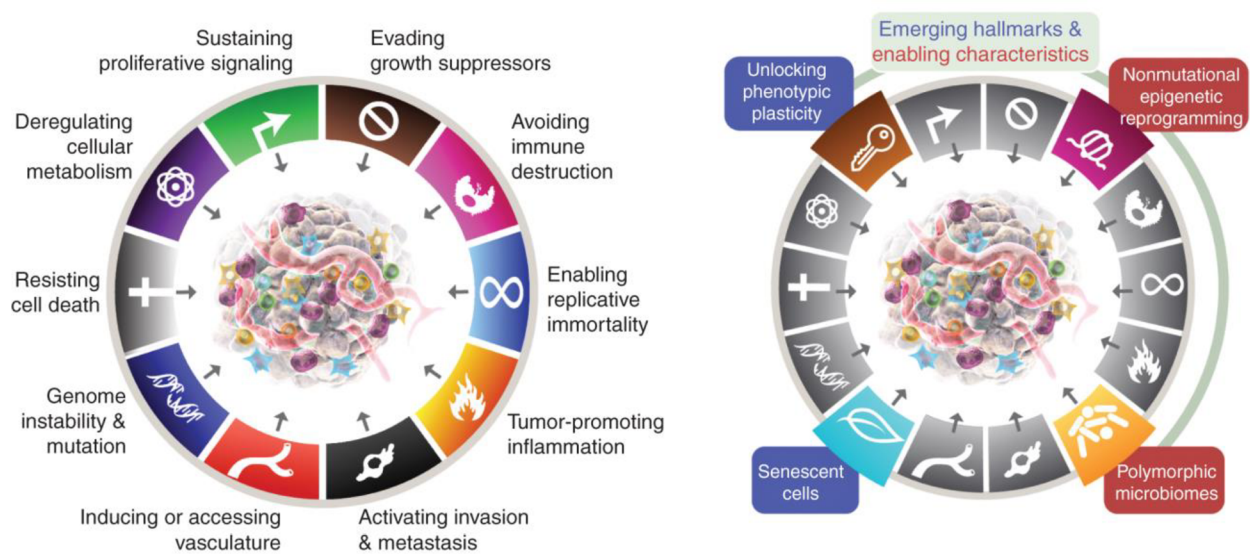


Figure 1: Depiction of the current model of hallmarks and enabling characteristics of cancer (reprinted from Hanahan, 2022).

1.1.6. Self-Sufficiency in Growth Signals

Normal cells need external mitogenic growth signals in order to proliferate. They rely on growth factors that bind cell surface receptors, supplied by the tissue microenvironment. Tumor cells do not depend on these signals. Many cancer cells can synthesize their own growth factors and stimulate their own growth factor receptors. This process is called *autocrine secretion* (Sporn & Todaro, 1980).

Furthermore, changes to growth signal receptors or downstream components such as Ras and Raf, two common oncogenes, can allow for constitutive activation of proliferative pathways independent of ligand binding. Deregulation of negative-feedback mechanisms allows cancer to proliferate rapidly (Hanahan, 2022; Hanahan & Weinberg, 2000).

1.1.7. Insensitivity to Anti-Growth Signals

Growth inhibitors prevent excessive proliferation by binding to surface receptors. A key pathway involves the retinoblastoma protein Rb, which determines whether a cell continues through its cell cycle. It can force the cell into quiescence or make it permanently postmitotic by interfering with transcription factors. This pathway can be disrupted in several ways, including mutation of the Rb gene, which permits unhindered proliferation. Another significant suppressor of cell growth and division is the p53 protein, which is also involved in apoptosis. The existence of two major effectors of growth inhibition provides a backup should one of the proteins be disrupted (Hanahan & Weinberg, 2000).

Another source of anti-growth signaling is contact inhibition. The proliferation of healthy cells is regulated by neighboring cells and the extracellular matrix (ECM). Merlin is a protein that promotes cell-cell adhesion through structural proteins like E-cadherin, preventing unwanted growth, and blunts exogenous growth signals by sequestering GF receptors. LKB1 acts to maintain epithelial structure and can oppose the Myc oncogene. Both NF2, the gene coding for Merlin and LKB1 have been implicated as tumor suppressor genes due to their absence in neoplastic growths (Hanahan & Weinberg, 2011).

1.1.8. Evading Apoptosis

In healthy tissues, damaged cells are eliminated via apoptosis to preserve the well-being of the organism. In response to stress, intracellular signals effect the self-destruction of the cell in a highly controlled manner. Cytochrome C released from the mitochondria or FAS, when apoptosis is mediated extrinsically, activates caspases that cause the breakdown of cellular components. These are then consumed by phagocytes. p53 is a major proapoptotic effector. It plays a crucial role in sensing DNA damage, oncogene signaling and hypoxia. The p53 gene is

defective in over half of human cancers. Still, due to the redundant nature of the apoptotic signaling cascade, parts of the pathway may remain intact in malignant cells. This indicates the possibility for novel therapeutic interventions in oncology. In contrast to apoptosis, in which the death of a cell is carried out systemically and its contents are taken care of, necrosis releases the cell's contents in an uncontrolled manner into its surroundings. The resulting inflammatory response creates a pro-tumor environment. It follows that the uncontrolled death of some cells, by evading apoptosis, in a proliferating mass actually confers a net benefit (Hanahan & Weinberg, 2000, 2011).

1.1.9. Limitless Replicative Potential

Gaining independence from external signals that govern growth and evading apoptosis are not enough to ensure the growth of tumor tissue. Virtually all mammalian cells excluding stem cells are intrinsically limited in their capacity to replicate. Normal cells stop dividing once their Hayflick limit is reached. This limit has been found to be 60-70 divisions in tissue cultures.

Telomeres prevent information loss caused by the inherent asymmetry in replication between the leading and lagging strand during DNA replication. The progressive shortening of telomeres eventually leads to cell senescence. If cells at this stage happen to replicate further, they enter a state called crisis where the genomic instability caused by the end-to-end fusion of chromosomes results in the cell's death. Cancer cells circumvent this by overexpressing telomerase, the enzyme that restores telomeres, or via a recombination-based mechanism in some cases. In doing so, cancer cells can maintain their telomeres, giving them unlimited replicative potential. It is worth noting that even in the absence of telomeres, oncogenes can still promote a tumorigenic environment. When p53 is absent, premalignant cells dividing past their Hayflick limit and entering crisis can undergo chromosomal breakage-fusion-bridge cycles that introduce further mutations into the genome. (Hanahan & Weinberg, 2000, 2011)

1.1.10. Sustained Angiogenesis

Proximity to blood vessels is essential for all cells to provide them with oxygen and nutrients and eliminate waste products. As a mass of cells, a tumor is inherently limited in its ability to develop past a certain size without a dedicated blood supply. Most of the development of human vasculature occurs during early development and angiogenesis occurs only transiently in adults. The sustained activation of this process is among the first acquired capabilities in many cancers. Cancer cells stimulate the growth of blood vessels by manipulating the balance of pro- and anti-angiogenic signalling molecules such as VEGF and TSP-1 that bind surface receptors on endothelial cells. There is evidence to suggest that the specific means to achieving sustained angiogenesis vary among cancer types. The emerging neovasculature is leaky and disorganized. The degree of vascularization can vary significantly among different tumors (Hanahan & Weinberg, 2000, 2011).

1.1.11. Tissue Invasion and Metastasis

The major cause of human cancer deaths is metastasis. The process of metastasis formation is a highly complex process with many nuanced outcomes that is not fully understood. The formation and subsequent behavior of cancer colonies strongly depends on the type of cancer and their environment. Several cellular events enabling this progression have been elucidated. Defects in proteins that promote cell-to-cell and cell-to-ECM adhesion allow tumors to invade neighboring tissue and metastasize. E-cadherin for instance is commonly found in epithelial cells and acts as a prominent safeguard against tumor growth and protects against the detachment and migration of cancer cells. Mutation, underexpression, or proteolysis of the protein results in invasion and metastasis. Metastatic cells can alter their integrin subunit

expression pattern to favor their new environment. An increase in extracellular protease activity improves a tumor's ability to invade other tissues (Hanahan & Weinberg, 2011).

1.1.12. Further Hallmarks

Also of note are an inherent instability in the genome and inflammation that promotes tumor growth. Safeguarding mechanisms against DNA damage are disrupted, leading to an increased rate of mutations. It has been shown that local inflammation can confer benefits to the growing tumor. Bioactive molecules released by immune cells such as growth factors, proangiogenic factors and reactive oxygen species promote tumor growth and give rise to other hallmark capabilities (Hanahan & Weinberg, 2011).

1.2. Glucose Metabolism and The Warburg Effect

Cells alter their manner of glucose metabolism depending on their rate of division. Namely, cells stimulated to proliferate will always opt for glycolysis, where large amounts of carbon are wasted. This holds true for unicellular organisms experiencing an abundance of nutrients as well as for cells of multicellular organisms stimulated to grow. Conversely, the respective absence of nutrients or growth signals compels the same cells to switch to oxidative metabolism. This common behavior suggests that nonoxidative metabolism is energetically more favorable during states of proliferation while oxidative metabolism is better during states of low nutrient supply. In aerobic conditions and in the absence of external growth stimuli, the mitochondria of differentiated cells metabolize the pyruvate produced during glycolysis using oxidative phosphorylation in the tricarboxylic acid cycle (TCA). This process is highly efficient and yields 36 mol ATP per mol glucose. It is only during a lack of oxygen that these cells instead rely on anaerobic glycolysis, in which pyruvate is reduced to lactate, yielding only 2 mol ATP

per mol glucose. O. Warburg found that this pathway paradoxically predominates in cancer cells even under aerobic conditions. This initially seems counterproductive due to the low output of ATP. However, there is no need to improve the efficiency of metabolism in a cell provided with excess nutrients. But a cell dividing at a high rate needs to optimize its energy turnover to maximize growth. Aerobic glycolysis displayed in neoplastic cells produces ATP at a comparatively fast rate. Additionally, a rapidly proliferating cell needs sufficient substrate to continue dividing. Instead of being oxidized to CO₂, the intermediates of glycolysis are used in anabolism. Glucose and glutamine are catabolized as sources of carbon and nitrogen (Heiden et al., 2009).

Nutrient uptake is usually externally regulated. In most healthy cells, the uptake of glucose from the bloodstream is insulin dependent. Binding of insulin to its receptor activates the phosphoinositide 3-kinase (PI3K) pathway, causing glucose transporter (GLUT) translocation downstream. Once inside the membrane, GLUT enables the passage of glucose into the cell (Świdarska et al., 2018). Oncogene signaling or mutations in its components can lead to a constitutive activation of the PI3K pathway. This causes GLUT translocation independent of insulin, leading the cancer cell to take up excessive amounts of glucose. Glycolysis is then increased significantly, and large amounts of lactate are excreted (Wise & Thompson, 2010). This effect can occur even in non-insulin dependent tissues. Expression of this pathway makes cells dependent on glucose; depriving the tumor of glucose causes it to regress (Heiden et al., 2009).

1.2.1. Glutamine Addiction

Glutamine plays multiple crucial roles in cancer cell metabolism, serving as an important source of NADPH. It is essential to the activation of the mammalian target of rapamycin (mTOR) through essential amino acids. In the synthesis of nonessential amino acids, it serves

as the source of nitrogen. Glutamine is consumed at rates far exceeding those of other amino acids in cancer cell lines. Figure 2 depicts the pathways involving glutamine relevant to oncology. After being converted to glutamic acid via glutaminase (GSA), it is subsequently turned into α -ketoglutarate, a TCA intermediate, serving as a mitochondrial substrate (Wise & Thompson, 2010). Similar to the excessive glucose uptake resulting in wasteful metabolism described above, oncogenic signaling from Myc can increase the uptake of glutamine into the cell by upregulating the glutamine transporter, followed by an upregulation of GSA. Many steps in the metabolism of glutamine in cancer cells ranging from the incorporation into the cell via the upregulated transporter to the various downstream glutaminolytic enzymes are possible pharmacologic targets in cancer therapy research. In the context of this thesis, GSA is of particular interest. (Wise & Thompson, 2010).

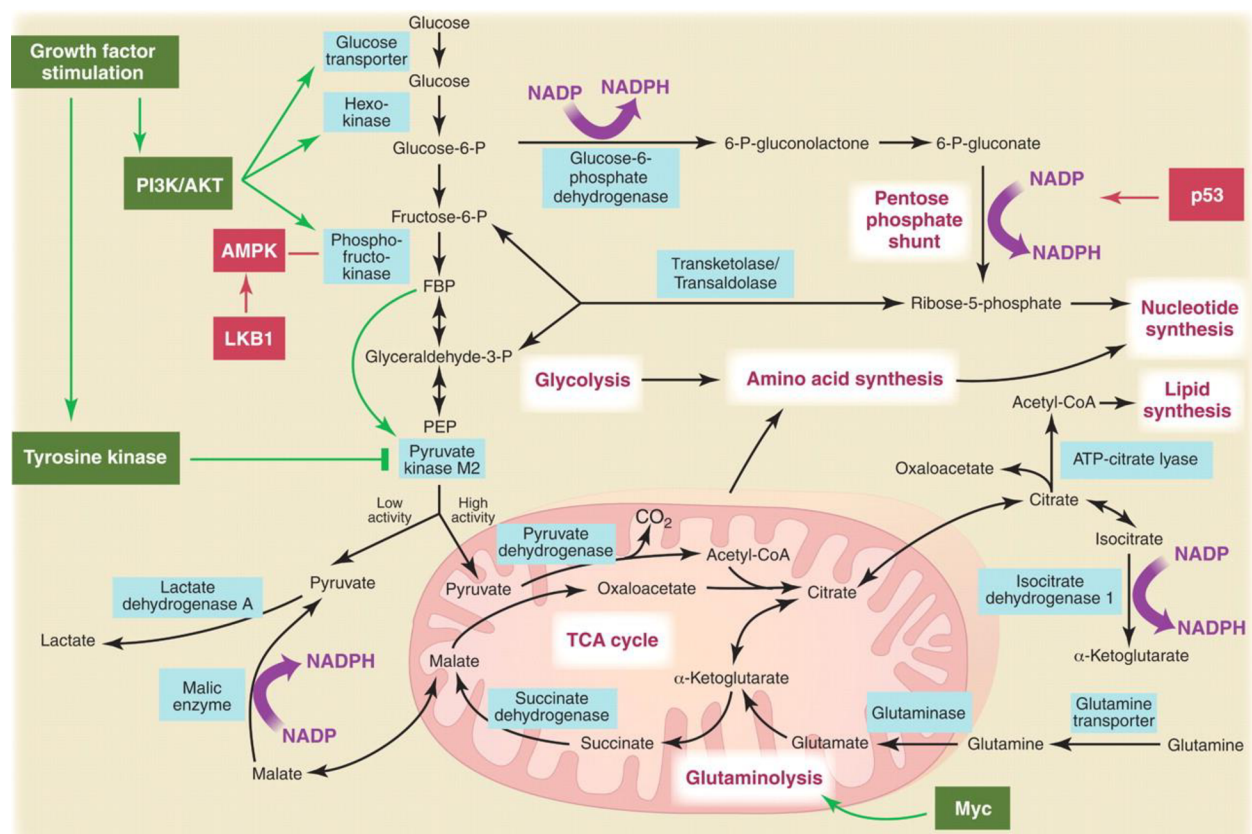


Figure 2: Connection of glycolysis, oxidative phosphorylation, the pentose phosphate pathway, and glutamine metabolism in proliferating cells (reprinted from Wise and Thompson, 2010).

1.3. Types of Cancer Therapy

The five pillars of treatment are surgery, radiation therapy, chemotherapy, immunotherapy, and targeted therapy (Oiseth & Aziz, 2017). Patients with advanced stages of cancer receive palliative care (WHO, 2022). This thesis is focused on two of them: chemotherapy and immunotherapy.

1.4. Chemotherapy

1.4.1. A History of Chemotherapy

The term was coined by Paul Ehrlich in the early 1900s, referring to the treatment of disease using chemicals. Although not free from controversy, Ehrlich is widely regarded as a pioneering figure in the fields of immunology and chemotherapy. He is known for his development of cell staining techniques, his cure for syphilis and his work on animal models for drug discovery (DeVita & Chu, 2008; Kaufmann, 2008). Ehrlich was in search of a “magic bullet”, an ideal therapeutic agent that would target malignant agents directly without harming healthy cells. (Strebhardt & Ullrich, 2008).

Advances in chemotherapy over the past century are marked by ever increasing specificity. The first class of drugs developed against cancer were nitrogen mustards. Initially used as chemical warfare agents in World War I, their antitumor effects were discovered accidentally when they were studied during World War II. Their ability to promote cancer regression was shown in both mice and humans, sparking research into related alkylating agents. The elucidation of the structure of DNA gave rise to new therapeutic vectors. Another breakthrough in chemotherapy following this discovery was the development of 5-fluorouracil in the 1950s. It was designed to interfere with a particular aberrant pathway of cancer cells, making it essentially a crude form of targeted therapy. At the time, the public was still skeptical of this emerging field, and the drugs were regarded as poison rather than medicine. Animal

models greatly improved during the 1960s, and therapies became increasingly effective. When it was shown that combination chemotherapy could cure acute childhood leukemia and advanced Hopkin's disease, public opinion shifted and research into adjuvant chemotherapy was started. In the 1990s, monoclonal antibodies (mAbs) like rituximab saw clinical applications. Findings in signal transduction pathways allowed for the development of targeted therapeutics like Imatinib, aimed at a specific tyrosine kinase. Development of other kinase inhibitors followed suit. Ehrlich's vision of the magic bullet can be said to have been realized due to the highly specific nature of the agents in use today. The complex nature of cancer means that therapeutic outcomes can be improved by a combination of treatments targeting multiple components of signal transduction and metabolism (DeVita & Chu, 2008; Strebhardt & Ullrich, 2008).

1.4.2. 6-diazo-5-oxo-L-norleucine

6-diazo-5-oxo-L-norleucine (**DON**) is a glutamine antagonist that has been studied since the 1950s. Its antitumor properties stem from its ability to interfere with the highly upregulated metabolism of glutamine-addicted tumors. Although initially promising, clinical trials were halted due to gastrointestinal toxicity. DON prodrugs have been investigated to circumvent this toxicity by preferentially targeting tumor tissue (Lemberg et al., 2018; Tenora et al., 2019).

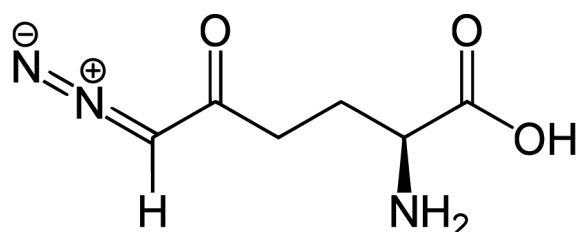


Figure 3: Structure of 6-diazo-5-oxo-L-norleucine (DON).

1.5. Immunotherapy

1.5.1. Immunity

The body's immune system is composed of nonspecific, innate immunity and specific, adaptive immunity working in tandem. Because the body is constantly exposed to pathogens, there must be mechanisms in place to protect against infection and disease.

Innate immunity is a host defense mechanism against microbes that is strongly conserved across organisms. Its first lines of defense against pathogens are protective endothelial linings, defensins and complement proteins. It can distinguish between self and non-self. Microorganisms exhibit characteristic structural motifs called pathogen-associated molecular patterns (PAMPs). Those include peptidoglycan, certain nucleic acids, and lipopolysaccharides (LPS). Recognition of PAMPs leads to an inflammatory response and opsonization for phagocytosis (Alberts et al., 2002; Chaplin, 2010).

The innate immune system detects PAMPs via germline-encoded pattern recognition receptors (PRRs). Toll-like receptors (TLRs) are a type of PRR which are expressed in immune cells such as macrophages and dendritic cells. They are classified into cell surface and intracellular TLRs. The Toll/IL-1 receptor (TIR) domain initiates downstream activation of transcription factors such as NF- κ B, which promote the release of proinflammatory cytokines and chemokines (Kawasaki & Kawai, 2014).

The **complement system** is a complex network of proteins that act in a coordinated cascade in response to pathogens. It can be activated in one of three major pathways: the classical, the alternate, and the lectin pathway. In the classical pathway, C1q binds to antibodies attached to the surface of a pathogen that form an immune complex. The lectin and alternate pathways are activated by mannose-binding lectin (MBL) or ficolins binding to specific carbohydrate patterns. Crucial to all three cascades is the formation of C3 and C5 convertases

to cleave their respective proteins and formation of the membrane attack complex (MAC) (Reis et al., 2019).

Key immune cells of the **innate immune system** include neutrophils, the most abundant white blood cells, macrophages which are involved in both innate and adaptive immunity, and natural killer (NK) cells that are crucial to defending against tumors and virus-infected cells (Marshall et al., 2018).

Phagocytosis is the detecting and engulfing of particles or microorganisms. After the particle is recognized by binding to PAMPs, a phagosome is formed around it. The phagosome then fuses with the cytoplasmic lysosome, forming a phagolysosome. After being degraded by lysing enzymes, the remains are expelled through exocytosis. Phagocytosis is performed by almost all cells to varying extents. Macrophages, neutrophils, monocytes, dendritic cells, and osteoclasts are so-called professional phagocytes (Uribe-Querol & Rosales, 2020).

B cells, T cells, NK cells and NK-T cells arise from the common lymphoid progenitor cells derived from the pluripotent hemopoietic stem cells of the bone marrow (Chaplin, 2010). The **adaptive immune response** is largely mediated through antigen-specific T and B lymphocytes. Innate immunity plays a part in activating these cells. T cells express a protein on their surface to bind to antigens presented by antigen presenting cells (APC). Although slow to respond upon initial exposure to a certain pathogen, the clonal expansion of T and B cells allows for immunologic memory to quickly mount an effective defense against the pathogen in the future (Chaplin, 2010).

The inflammatory response is largely mediated through cytokines. Interleukin-1 (IL-1), interleukin-6 (IL-6), and tumor necrosis factor (TNF- α) are important signaling molecules in promoting inflammation. Proinflammatory chemokines such as interleukin-8 (IL-8) are produced by cells in order to promote chemotaxis, the migration of leukocytes towards a site of infection (Turner et al., 2014).

Immune cells such as effector T cells must be trained to be able to respond to a certain antigen. This is mediated through APC which include dendritic cells, B cells, and macrophages among others. They present antigens obtained from phagocytosis in major histocompatibility complex (MHC) molecules on their surface, express costimulatory molecules and secrete cytokines and chemokines (Eiz-Vesper & Schmetzer, 2020).

1.5.2. Approaches in Immunotherapy

Tumor remission following bacterial infection has been observed for centuries. W. Coley was among the first to document the phenomenon in the late 1800s (William B. Coley, 1893). Elucidation of PAMPs led to the development of synthetic TLR agonists, which on their own did not perform as expected (Guha, 2012).

Chimeric antigen receptor (CAR)-T cell therapy (Sternier & Sternier, 2021), checkpoint inhibitors (Johnson et al., 2022), and cytokines (Conlon et al., 2019) are among common approaches in immunotherapy.

Monoclonal Antibodies (mAbs) have become a staple of immunotherapy for a variety of pathologies including cancer. The development of human mAbs has led to improved outcomes and safety profiles in therapy (Singh et al., 2018).

Chimeric antigen receptor (CAR)-T cell therapy (Sternier & Sternier, 2021), checkpoint inhibitors (Johnson et al., 2022), and cytokines (Conlon et al., 2019) are among common approaches in immunotherapy.

1.6. MBTA Therapy

MBTA is an abbreviation for the therapeutic mixture of mannan-BAM, resiquimod (R-848), polyinosinic-polycytidylic acid (poly(I:C)), lipoteichoic acid (LTA) and anti-CD40 (Caisová et al., 2018). Intratumoral application of this combination therapy has proven effective in

mouse models of pancreatic adenocarcinoma. Simultaneous activity of innate and adaptive immunity leads to phagocytosis of tumor cells and a specific adaptive immune response. Most mice show remission of the tumor, resistance to re-transplantation and metastasis (Medina et al., 2020; Uher et al., 2021).

1.6.1. Mannan-BAM

The abbreviation **BAM** stands for *biocompatible anchor for cell membranes*. This molecule consists of two parts. The first part is a hydrophobic oleic acid chain, which can pass through the cell membrane without breaking it and remain embedded in it. This way, it serves as an anchor. The second part is a hydrophilic polyethylene glycol (PEG) with an attached reactive group where other molecules (**mannan** in our case) can be covalently bounded (Kato et al., 2004).

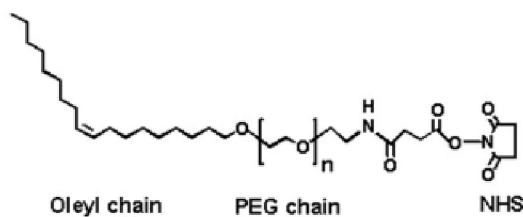


Figure 4: Structure of the BAM molecule (reprinted from Kato et al., 2004).

Mannan is a polysaccharide consisting mainly of mannose. Multiple types exist and are classified as PAMPs of fungi and Gram-negative bacteria (Lipke & Ovalle, 1998).

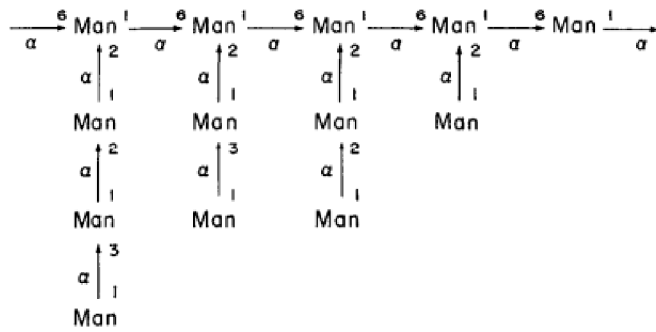


Figure 5: General schema of the structure of mannan (reprinted from Lipke and Ovalle, 1998).

Mannan-BAM anchors to the membrane of tumor cells via BAM and is recognized by mannan-binding lectin (MBL) (Janeway & Medzhitov, 2002), which leads to activation of the complement system through the lectin pathway. A chain reaction is triggered, resulting in the marking of mannan-BAM-anchored cells by iC3b molecules. This process is called opsonization. iC3b molecules are recognized by CR3 receptors on the surface of innate immune cells (phagocytes, NK cells). As a result, innate immune cells can attack and eliminate opsonized tumor cells (Janotová et al., 2014; Waldmannová et al., 2016). This not only weakens the tumor, but also releases antigens, which can be used to train adaptive immune cells.

1.6.2. TLR Agonists

The MBTA therapeutic mixture contains three TLR agonists – lipoteichoic acid (**LTA**), resiquimod (**R-848**), and **poly(I:C)**. Their function is the induction of pro-inflammatory cytokines, which leads to inflammatory infiltration into the tumor. They act synergistically, improving the therapeutic effect of the mixture.

LTA originates from the cell wall of Gram-positive bacteria. It is recognized by TLR2, which leads to the activation of innate immune cells and their subsequent expression of inflammatory cytokines (TNF- α , IL-1 β , IL-6, IL-12) (Takeuchi et al., 1999). IL-12 is an

important cytokine linking innate and adaptive immunity, as well as an important growth factor of T cells (Hessle et al., 2000). LTA in MBTA is derived from *Bacillus subtilis* (Caisová et al., 2018).

Another MBTA component, **R-848** (resiquimod), is derivative of imiquimod (R-837) (Weeks & Gibson, 1994). R-848 is recognized by murine and human cells via TLR7 (Hemmi et al., 2002), and in humans also by TLR8 (Jurk et al., 2002). R-848 aids in the maturation of dendritic cells and strongly induces the transcription factor NF- κ B and the secretion of pro-inflammatory cytokines such as TNF- α , IL-6, and IFN I (Ahonen et al., 2004; Gutterman, 1994; Hemmi et al., 2002; Weeks & Gibson, 1994). In synergy with poly (I:C), it induces significant IL-12 expression (Napolitani et al., 2005).

Poly(I:C) is a TLR3 ligand that induces the production of pro-inflammatory cytokines capable of promoting adaptive immunity (Zhu et al., 2007). It is a potent inducer of IFN- α , which is the dominant driver of two innate cellular responses: dendritic cell maturation and activation of NK cells to produce IFN- γ . Mature dendritic cells present antigens to naïve CD4+ and CD8+ T lymphocytes in lymph nodes, engaging adaptive immunity (Talmadge et al., 1985).

R-848 and poly(I:C) work together with **anti-CD40 antibody** in strong synergy producing IL-12 (Napolitani et al., 2005).

1.6.3. Anti-CD40 Antibody

The final component of the therapeutic mixture is an **anti-CD40 agonistic antibody**. It is a member of the tumor necrosis factor receptor family – a ligand for the CD40 receptor. It is expressed on the surface of dendritic cells (and other APCs). Activation of CD40 promotes inflammation and the activation of T and NK cells (Hassan et al., 2014). By binding to the receptor, the dendritic cell matures and is stimulated (Kooten & Banchereau, 2000). Activated mature APCs internalize tumor antigens and present them to naive T cells in lymph nodes,

which leads to an effective T cells-based anti-tumor response (Shurin, 1996; Paglia et al., 1996; Bennett et al., 1998).

In addition, the synergy of R-848, poly(I:C), and anti-CD40 leads to the expansion of CD8+ T cells producing IFN- γ and the formation of memory cells, and the immune response is 10-20 times higher than when using anti-CD40 alone. At the same time, R-848 and poly(I:C) stimulate the production of IFN- α and IFN- β , whereby in the presence of anti-CD40 antigens are cross-presented to naïve CD8+ lymphocytes and not only cytotoxic T cells, but also a significant amount of memory CD8+ cells (Ahonen et al., 2004).

1.6.4. Limitations of MBTA and DON Therapies

There is a big disadvantage to MBTA therapy. It has to be injected directly into the tumor. Of course, thanks to that, it works against the specific tumor in which MBTA is applied. We also do not need such large dosages, which reduces side effects. On the other hand, if a tumor is badly accessible, it is not curable this way. The same applies to the case of facing too many or too small metastases. There are also situations where we do not know the location of all tumors in the body. Immunotherapies are generally also limited by the capabilities of the immune system.

The efficacy of DON increases with dose, but so do its side effects. With intratumoral application, a smaller dose is needed than when given systemically, but according to our findings, i.p. is the best way to apply DON (Danielová, 2022).

We are looking to replace mannan-BAM going forward. Since mannan is an unspecified polymer from the yeast surface and does not meet GMP (good manufacturing practice) requirements for clinical trials, fMLF (see below) is being explored as a substitute (Janotová et al., 2014).

1.7. fMLF

fMLFG5K10STE (from here on referred to as fMLF) is a synthetic peptide with the sequence of Formyl-MLFGGGGGK(K(Ste))-NH₂. K(Ste) refers to a lysine amino acid with a stearyl group attached to its sidechain (the epsilon amino group). The C-terminal of this lysine is in the amide form. Activation of formyl peptide receptors (FPRs) promotes chemotaxis of phagocytes and the inflammatory response (He & Ye, 2017).

The molecule is inspired by N-Formylmethionyl-leucyl-phenylalanine, an N-formylated tripeptide derived from bacteria. It is very effective at promoting chemotaxis and activating macrophages (Panaro & Mitolo, 1999).

fMLF consists of two ends and a spacer containing 10 lysine residues. The positively charged spacer is designed to be attracted to tumor cells, which are negatively charged. This improves the specificity of the molecule in theory (Ženka, Lencová, oral communication).

2. Aims

- Based on the literature review, this thesis's first goal was understanding the principles and limitations of DON and MBTA therapy.
- The second purpose of the thesis was to process and statistically evaluate data from two experiments obtained by Tumor Therapy Laboratory team members.
- Another goal was to learn the use of MBTA therapy in practice. The experiment aimed to determine whether replacing mannan-BAM in the MBTA therapeutic mix is possible.
- The last task was to develop the discussion based on this research and the research of a wider circle of team members.

3. Materials and Methods

3.1. List of Chemicals

Table 1: List of chemicals and their sources.

Substance	Source/Supplier
Anti-Mouse CD40, clone FGK4.5/FGK45	BioXCell, USA
BAM – Biocompatible anchor for cell membrane, Mw 4000	NOW, Belgian
Chitosan glutamate – catalog number 54041	HMC+, Germany
DMEM – Dulbecco’s modified eagle medium	VWR, USA
DMSO – Dimethyl-sulfoxide	Sigma-Aldrich, USA
DON – 6-diazo-5-oxo-L-norleucine	synthesized by Dr. Pavel Majer, Institute of Organic Chemistry and Biochemistry of the Czech Academy of Sciences
EDTA – Ethylenediamine tetra acid	Sigma-Aldrich, USA
FCS – Fetal calf serum	VWR, USA
fMLFG5K10STE	Schafer-N, Denmark
HBSS – Hank's balanced salt solution	Sigma-Aldrich, USA
JHU-083 – ethyl(S)-2-((S)-2-amino-4-methylpentanamido)-6-diazo-5-oxohexanoate	synthesized by Dr. Pavel Majer, Institute of Organic Chemistry and Biochemistry of the Czech Academy of Sciences
LTA – Lipoteichoic acid, Bacillus subtilis	Sigma-Aldrich, USA
Mannan – Saccharomyces cerevisiae	Sigma-Aldrich, USA
Matrigel	Sigma-Aldrich, USA
PBS – Phosphate-buffered saline	VWR, USA
Poly(I:C) – Polyinosinic-polycytidylic acid, sodium salt	Sigma-Aldrich, USA
R-848 – Resiquimod	Tocris Bioscience, UK
Trypan blue – 0.5% in H ₂ O	Sigma-Aldrich, USA
Trypsin	Sigma-Aldrich, USA

3.2. Preparation of Chemicals

3.2.1. Manan-BAM

First, reductive amination of mannan was performed, and then the solution was reduced for five days with sodium cyanoborohydride in ammonium acetate - pH 7.5, temperature 50 °C.

The resulting solution was allowed to dialyze overnight against PBS at 4 °C through a

MWCO3500 dialysis membrane (Serva, Heidelberg). The result was a mannan-NH₂ solution whose pH value had to be maintained between 7.2 and 8.5.

Subsequently, a solution of BAM₄₀₀₀ in DMSO (7.3 mM) was prepared and added to the mannan-NH₂ solution in an equimolar ratio. This mixture was allowed to react for two hours (room temperature). The reaction was stopped by adding TRIS/HCl (pH 8.0). Subsequently, the solution was dialyzed using the same procedure as before. The resulting solution was 0.2 mM mannan-BAM in PBS, which was kept frozen at -20 °C until use. All solutions used were sterilized by filtration (pore diameter 0.22 μm).

3.2.2. MBTA Mixture and its Modifications

- **Basic immunotherapeutic mixture mannan-BAM + R-848 + poly(I:C) + LTA + anti-CD40 (MBTA)**

A solution was made of 0.5 mg R-848 (hydrochloride first made using an equivalent of 3.5% HCl) + 0.5 mg poly(I:C) + 0.5 mg LTA + 0.4 mg anti-CD40 per 1 mL 0.22 mM mannan-BAM in PBS. This was followed by filtration sterilization (0.22 mM), aliquoting and freezing.

- **R-848 + poly(I:C) + LTA + anti-CD40 (TA)**

5.65 mL PBS, 3 mg R-848 diluted in 8.4 μL 3.5% HCl and 75 μL PBS, 3 mg poly (I:C), 3 mg LTA, and 0.28 mL of 0.4 mg/mL anti-CD40

- **R-848 + poly(I:C) + LTA + anti-CD40 (TA) + 0.2 mM fMLFG5K10STE (fMLF)**

The treatment for group consisted of 5.65 mL 0.22 mM fMLF containing 2.72 mg fMLF in 5.65 mL PBS, 3 mg R-848 in 8.4 μL 3.5% HCl and 75 μL PBS, 3 mg poly(I:C), 3 mg LTA, and 0.28 mL of the 0.4 mg/mL anti-CD40 solution in 12 injections of 0.5 mL.

- **R-848 + poly(I:C) + LTA + anti-CD40 (TA) + 1 mM fMLFG5K10STE (fMLF)**

Group H was similar to the previous one with a higher fMLF dose. 5.65 mL 1.1 mM fMLF containing 13.6 mg fMLF in 5.65 mL PBS, 3 mg R-848 in 8.4 µL 3.5% HCl and 75 µL PBS, 3 mg poly(I:C), 3 mg LTA, and 0.28 mL of the 0.4 mg/mL anti-CD40 solution were given in 12 injections of 0.5 mL.

3.2.3. 6-diazo-5-oxo-L-norleucine (DON)

- DON was administered as a solution of different concentrations in PBS.
- In experiment II, DON was administered as a solution of concentration 3.08 mg/mL 1.5% chitosan glutamate.
- In experiment II, DON was administered as a solution of concentration 3.08 mg/mL 50% Matrigel. It was kept on ice until application.
- JHU-083 was administered as a solution of concentration 2.81 mg/mL PBS.

3.2.4. Mixture for Trypsinization of Cultivated Cells

A trypsinization mixture consisting of 0.02% EDTA in HBSS and 0.25% trypsin was used to release the adhered cells.

3.3. Mice

The experimental procedures were conducted on female C57BL/6 murine strain, obtained from Charles River Laboratories for the first and second experiment, and from AnLab for the third experiment at the age of 9 weeks (arrived at 8 weeks old and were acclimatized for a week). The mice weighed approximately 20 g and were housed in individually ventilated cages (IVCs) with a stable temperature of 22 °C and an air humidity of 65%. The photoperiod was set to 12

hours of light and 12 hours of darkness. The mice were provided with unlimited access to sterile feed pellets and sterile distilled water. All experiments were performed *in vivo*.

3.4. Cell Line and Cultivation

The Panc02 mouse pancreatic adenocarcinoma cell line was donated by Professor Lars I. Partecke from the University of Greifswald in Germany. The cells were cultured in Dulbecco's Modified Eagle Medium (DMEM) supplemented with 10% FCS, penicillin (100 U/mL), streptomycin (100 µg/mL), amphotericin B (0.25 µg/mL), L-glutamine (2.2 mM), and mercaptoethanol (50 µM). The cells were maintained at a constant temperature of 37 °C in a 5% CO₂ atmosphere with saturated water vapor.

3.4.1. Preparation of Panc02 Cells for *In Vivo* Experiments

After sufficient cell growth, the culture medium was removed, and the cells were washed three times with sterile phosphate buffered saline (PBS). Trypsinization solution (0.02% trypsin and 0.25% EDTA in HBSS) was added to the adherent cells. The cells were then returned to the incubator, which was set at 37 °C and 5% CO₂ for 5 minutes to allow them to detach. The trypsinization reaction was stopped by adding DMEM medium with 10% FCS. The prepared cells were transferred to 50 mL tubes and counted in a Bürker chamber after staining with trypan blue. Subsequently, the cell concentration was adjusted to the desired level.

3.4.2. Transplantation of Panc02 Cells

Before the transplantation procedure, the mice were shaved on the corresponding flank. Subsequently, a subcutaneous injection of 100 µL of Panc02 cell suspension in serum-free DMEM containing 400,000 Panc02 cells was administered to this area. The same process was

repeated on the other flank to create a two-tumor model with a total of 2 x 400,000 Panc02 cells for experiments I and II. For the third experiment, only the right flank was injected.

3.5. Measurement of Tumors

From day zero inclusive, tumor sizes were measured (by digital caliper) every two days from day 0 to day 30. From the two measured values A and B, value A represents the diameter of the tumor in the longest part and value B the height of the tumor in the highest part. The volume of the tumor was subsequently calculated according to the formula:

$$V = \frac{\pi}{6} \cdot A \cdot B^2$$

The mean tumor volume for the entire group was calculated from the resulting tumor volumes of individual mice.

3.5.1. Calculation of Tumor Growth Reduction

The mean reduction in tumor growth was calculated using the formula:

$$x = \frac{\emptyset V_{control} - \emptyset V_{treated} \cdot 100}{\emptyset V_{control}}$$

where $\emptyset V_{control}$ is the mean tumor volume of the control group and $\emptyset V_{treated}$ means the mean tumor volume of the treated group. The resulting value was expressed as a percentage.

3.5.2. Calculation of the Area Under the Curve (AUC)

AUC is calculated as the sum of trapezoids. The following formula was used for the calculation:

$$x = \frac{V_{day_n} + V_{day_{n+2}}}{2} \cdot (day_{n+2} - day_n)$$

This formula can be further simplified by mathematical modifications:

$$x = V_{day_n} + V_{day_{n+2}}$$

For each mouse, x was calculated for all days, then it was added, and the results were averaged within the groups. For graphical representation, this value was divided by the value that was the highest within all groups and then multiplied by one hundred. The results are then in percentages and the highest value is 100%.

3.5.3. Statistical evaluation

Microsoft Excel 2016 and Statistica 4, StatSoft, Inc., were used to create graphs and statistically evaluate the measured values. The tests used in the Statistica program were one-way ANOVA with Tukey post-hoc test and Kaplan-Mayer plot with survival analysis by Log-rank test. Error bars indicate the standard error of the mean (SEM).

3.6. Schemas of Experiments

3.6.1. Experiment I – DON Dose Escalation Study

An experiment was conducted by Frejlachová, Skaličková, and Lencová.

20 days after the transplantation of Panc02 tumor cells on both flanks, mice with tumors were randomized into four groups of six (day 0). Mice were each placed in their own IVC box.

Day zero was also the day when the therapy started. All groups were treated by MBTA in four pulses, with three injections in each pulse. The mixture was injected in one pulse three days in a row, followed by a five-day break: 0, 1, 2; 8, 9, 10; 16, 17, 18; and 24, 25, 26. Therapeutic substances were administered intratumorally (50 μ L/mouse each time).

On day 1, DON therapy with different regimens started. A complete overview of the therapy is included in the table below (Tab. II).

Changes in tumor size and survival of mice (up to day 120) were monitored. These data were evaluated in this thesis.

Table II: Dosing regimen for the first experiment.

Group	Right Tumor	Days	Systemic Application	Days
A	MBTA	0, 1, 2, 8, 9, 10, 16, 17, 18, 24, 25, 26	DON i.p. 100 μ L 4 mg/mL	5, 13, 21, 29, 37
B	MBTA	0, 1, 2, 8, 9, 10, 16, 17, 18, 24, 25, 26	DON i.p. 100 μ L 4 mg/mL	5, 6, 13, 14, 21, 22, 29, 30, 37, 38
C	MBTA	0, 1, 2, 8, 9, 10, 16, 17, 18, 24, 25, 26	DON i.p. 100 μ L 4 mg/mL	5, 6, 7, 13, 14, 15, 21, 22, 23, 29, 30, 31, 37, 38, 39
D	PBS	0, 1, 2, 8, 9, 10, 16, 17, 18, 24, 25, 26	PBS i.p. 100 μ L	5, 13, 21, 29, 37

3.6.2. Experiment II – Optimization of DON Administration and Monitoring of Side Effects

An experiment was conducted by Skaličková, Danielová, and Lencová.

12 days after transplantation of Panc02 tumor cells on both flanks, mice with tumors were randomized into nine groups of six (day 0). Mice were each placed in their own IVC box.

Day zero was also the day when the mice therapy was started. All groups were treated by MBTA in four pulses, with three injections in each pulse. The mixture was administered intratumorally (50 μ L/mouse each time) following the schema below (Tab. III).

On day 1, therapy through glucose metabolism inhibition with different regimens and in different matrices started. A complete overview of the therapy is included in the table (Tab. III).

Changes in tumor size and survival of mice up to day 120 were monitored. Groups A, C, D, H, and I (Tab. III) were already evaluated by Mgr. Skaličková (2020) in her diploma

thesis. Groups E, H, and I (Tab. III) were already evaluated by Mgr. Danielová (2022) in her diploma thesis. Groups B, F and G are added to this thesis.

Other data from this experiment obtained by Mgr. Lencová were: mouse weights over time, food consumption, and water consumption (until day 61). The data are evaluated in this thesis.

Table III: Treatment regimen for the second experiment.

Group	Right tumor 50 μ L	Days	Glutamine metabolism inhibition	Days
A	MBTA	0, 1, 2; 8, 9, 10; 16, 17, 18; 24, 25, 26	DON i.p. 100 μ L 4 mg/mL	1, 8, 15, 22, 29
B	MBTA	0, 1, 2; 8, 9, 10; 16, 17, 18; 24, 25, 26	DON s.c., behind the neck 200 μ L 4 mg/mL	1, 8, 15, 22, 29
C	MBTA	0, 1, 2; 8, 9, 10; 16, 17, 18; 24, 25, 26	DON i.p. 100 μ L 1.54 mg/mL	1, 5, 9, 13, 17, 21, 25, 29
D	MBTA	0, 1, 2; 8, 9, 10; 16, 17, 18; 24, 25, 26	JHU-083 i.p. 100 μ L 2.81 mg JHU-083/mL	1, 5, 9, 13, 17, 21, 25, 29
E	MBTA	0, 1, 2; 8, 9, 10; 16, 17, 18; 24, 25, 26	DON i.t. - left 50 μ L 3.08 mg/mL	1, 5, 9, 13, 17, 21, 25, 29
F	MBTA	0, 1, 2; 8, 9, 10; 16, 17, 18; 24, 25, 26	DON i.t. - left 50 μ L 3.08 mg/mL In 1.5% chitosan glutamate	1, 5, 9, 13, 17, 21, 25, 29
G	MBTA	0, 1, 2; 8, 9, 10; 16, 17, 18; 24, 25, 26	DON i.t. - left 50 μ L 3.08 mg/mL In 50% Matrigel	1, 5, 9, 13, 17, 21, 25, 29
H	MBTA	0, 1, 2; 8, 9, 10; 16, 17, 18; 24, 25, 26		
I	PBS	0, 1, 2; 8, 9, 10; 16, 17, 18; 24, 25, 26		

3.6.3. Experiment III – Exploring the Substitution of Mannan-BAM with fLMF

Panc02 cells were applied on the right flank on day “-12”. In day “0”, mice were divided into 8 groups (8 mice per group) and placed in IVC box one by one.

In day zero also therapy started. All groups were treated in four pulses, with three injections in each pulse. The mixture was administered intratumorally (50 μ L/mouse each time) following the schema below (Tab. IV).

Changes in tumor size and survival of mice up to day 120 were monitored.

Table IV: The schema of third experiment

Groupe	Tumor – application of 50 μL	Days	Mice
A	MBTA	0,1,2; 8,9,10; 16,17,18; 24,25,26	8
B	TA	0,1,2; 8,9,10; 16,17,18; 24,25,26	8
C	0.2 mM mannan-BAM	0,1,2; 8,9,10; 16,17,18; 24,25,26	8
D	0.2 mM fMLFG5K10STE	0,1,2; 8,9,10; 16,17,18; 24,25,26	8
E	1 mM fMLFG5K10STE	0,1,2; 8,9,10; 16,17,18; 24,25,26	8
F	0.2 mM fMLFG5K10STE + TA	0,1,2; 8,9,10; 16,17,18; 24,25,26	8
G	1 mM fMLFG5K10STE + TA	0,1,2; 8,9,10; 16,17,18; 24,25,26	8
H	PBS	0,1,2; 8,9,10; 16,17,18; 24,25,26	8

4. Results

4.1. Experiment I

4.1.1. Tumor volumes

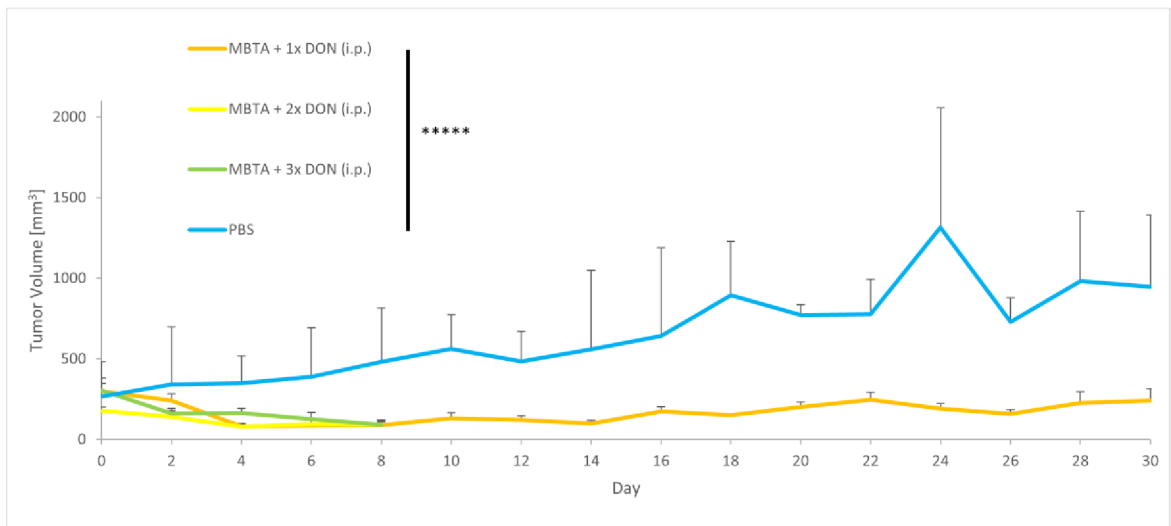


Figure 6: Right tumor volume over time in experiment 1. ***** $p \leq 0.0005$

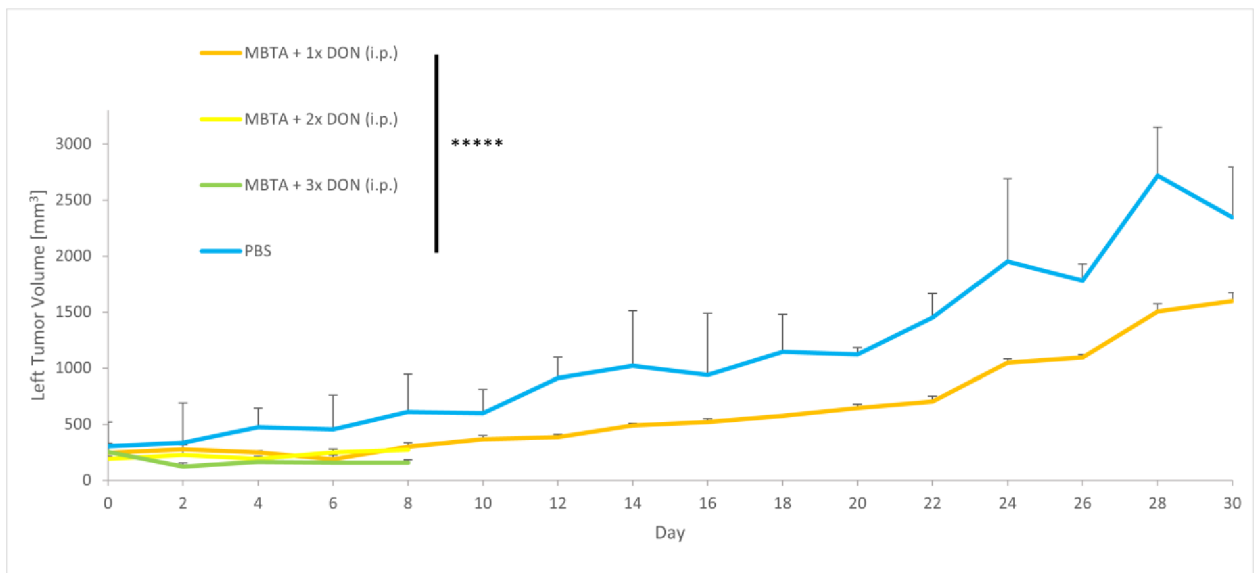


Figure 7: Left tumor volume over time in experiment 1. ***** $p \leq 0.0005$

Experiment 1 compared different dosages of DON. Area under the curve (AUC) was taken to evaluate statistical significance. Due to all subjects in groups B and C dying before the experiment ended, sufficient data could not be collected, and no statistically significant

difference could be established. The data collected are included in figures 6 and 7 for reference. Treatment in group A showed a clear attenuation in tumor growth compared to control ($p \leq 0.0005$). Tumors in the control group got increasingly larger over time while growth in group A stagnated.

4.1.2. Survival

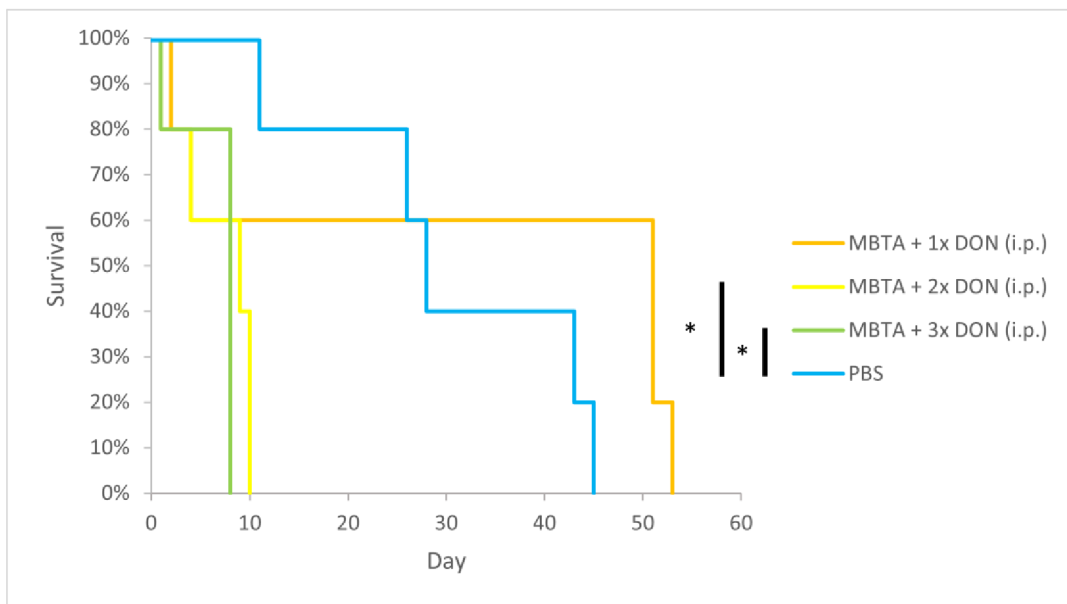


Figure 8: Survival for experiment 1. * $p \leq 0.05$

The graph in figure 8 depicts the survival analysis of the first experiment. There was a significant difference ($p \leq 0.05$) between the higher dosed groups, B and C, and control. Treatment with DON at higher dosed killed the mice prematurely, faster than a cancer would. Survival time was not significantly extended, and all mice died before the intended observation period of 120 days.

4.2. Experiment II

4.2.1. Tumor volumes

Here different routes of administration were explored. Figures 9 and 10 show tumor growth between the different groups on both flanks, respectively. The PBS control group

expectedly experiences the highest growth compared to the other groups. The administration of MBTA/PBS on the right side resulted in the inhibition of tumor growth in that particular group, whereas substantial growth was observed in the tumors on the left side.

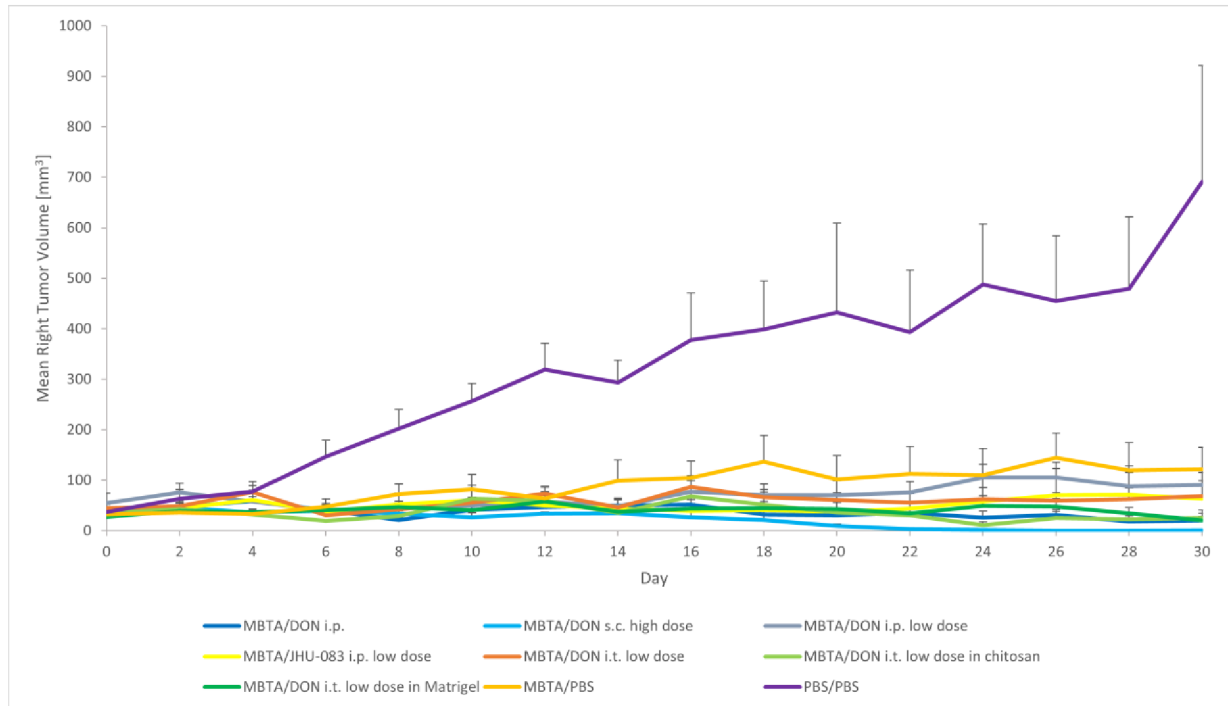


Figure 9: Right tumor growth for experiment 2.

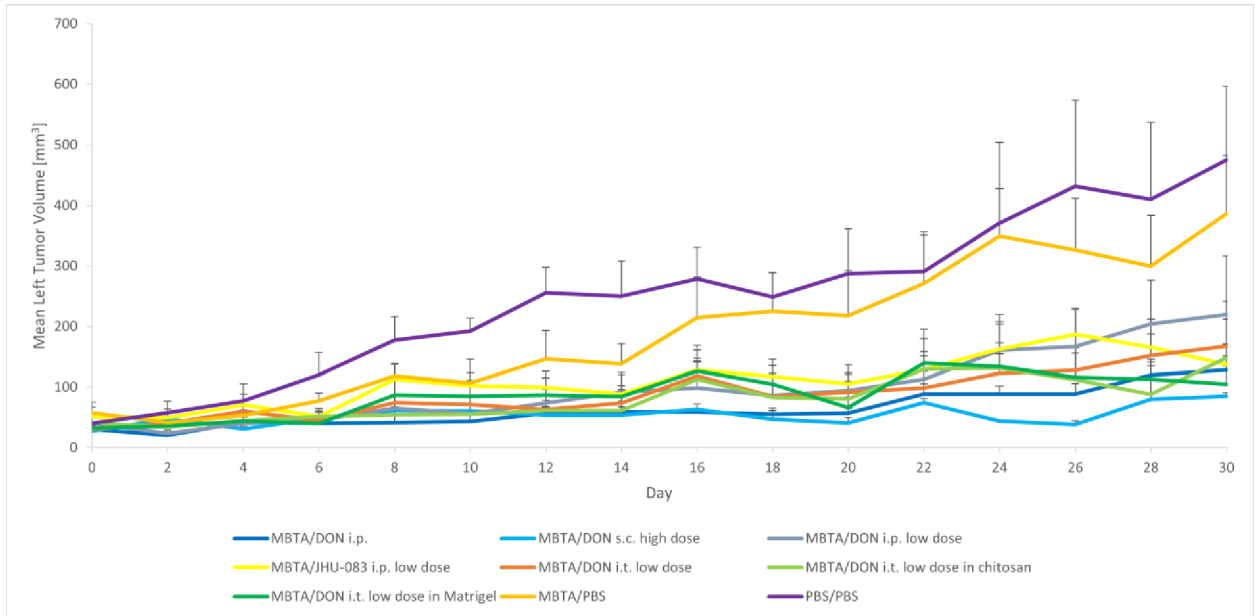


Figure 10: Left tumor growth for experiment 2.

AUC for tumor growth on both sides was calculated and a Tukey HSD test was performed to evaluate differences between the groups. For tumors on the right, groups A, B, D, F, and G differed significantly from control as depicted in figure 11. Figure 12 shows the AUC comparisons for the left tumors, where only subcutaneous administration of DON differed significantly from control.

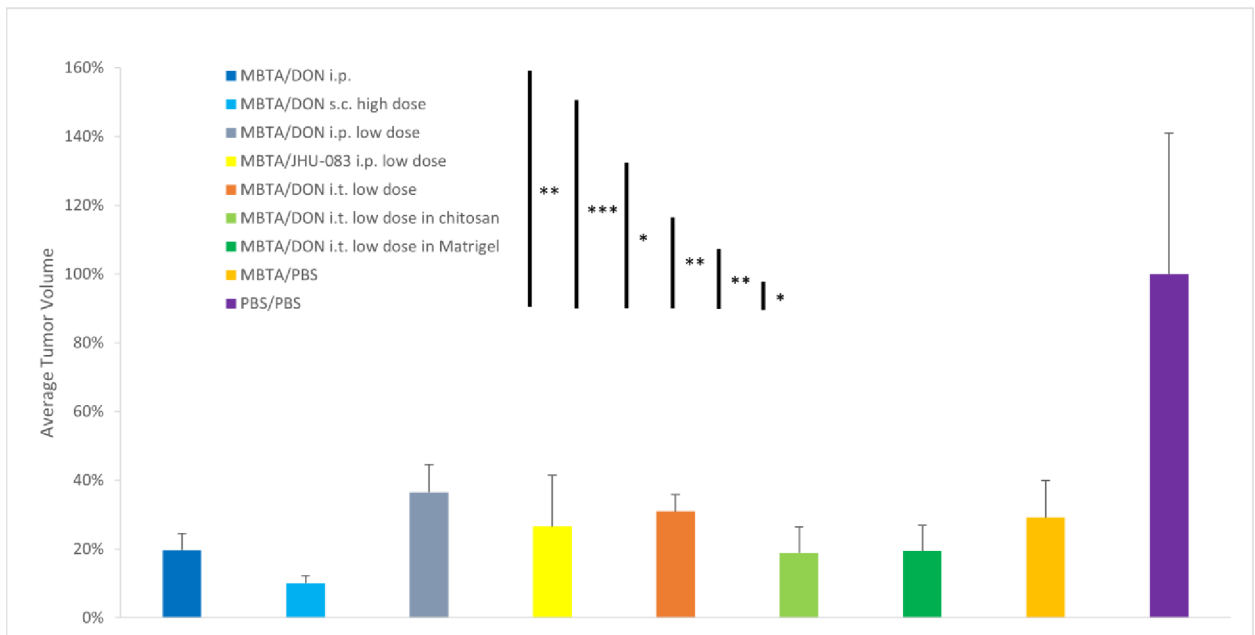


Figure 11: Right side AUC comparison for tumor growth in experiment 2. * $p \leq 0.05$, ** $p \leq 0.01$, *** $p \leq 0.005$

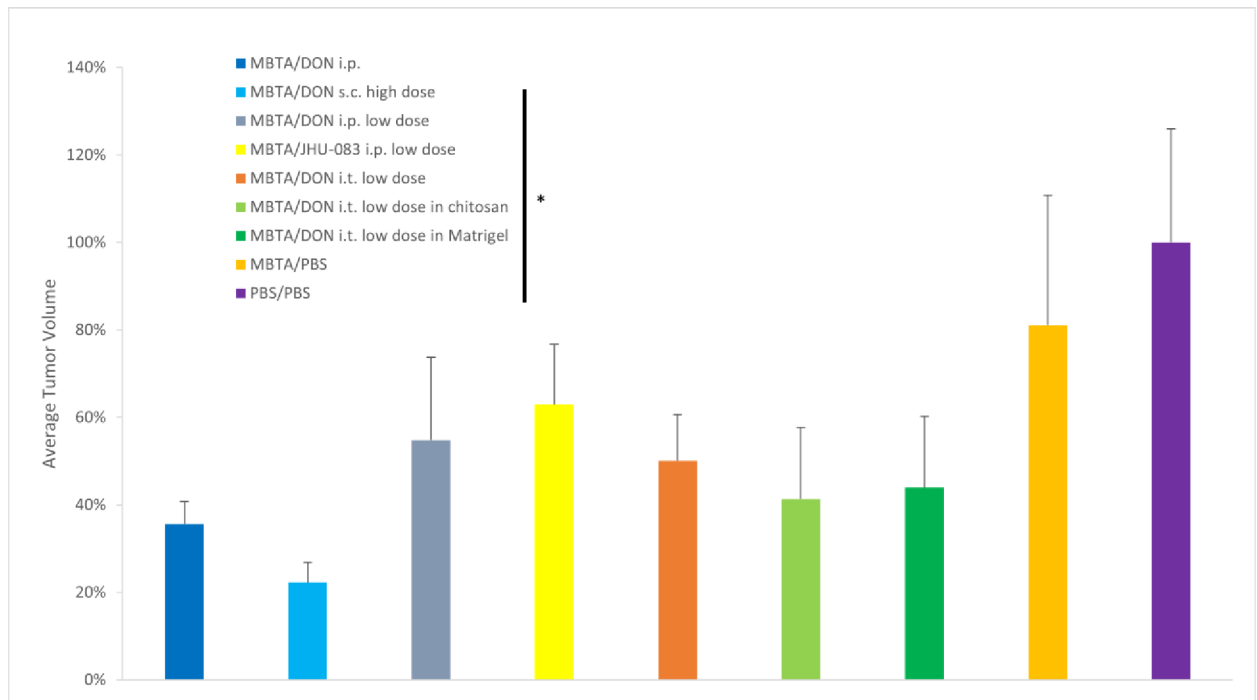


Figure 12: Left side AUC comparison for tumor growth in experiment 2. * $p \leq 0.05$

4.2.2. Survival

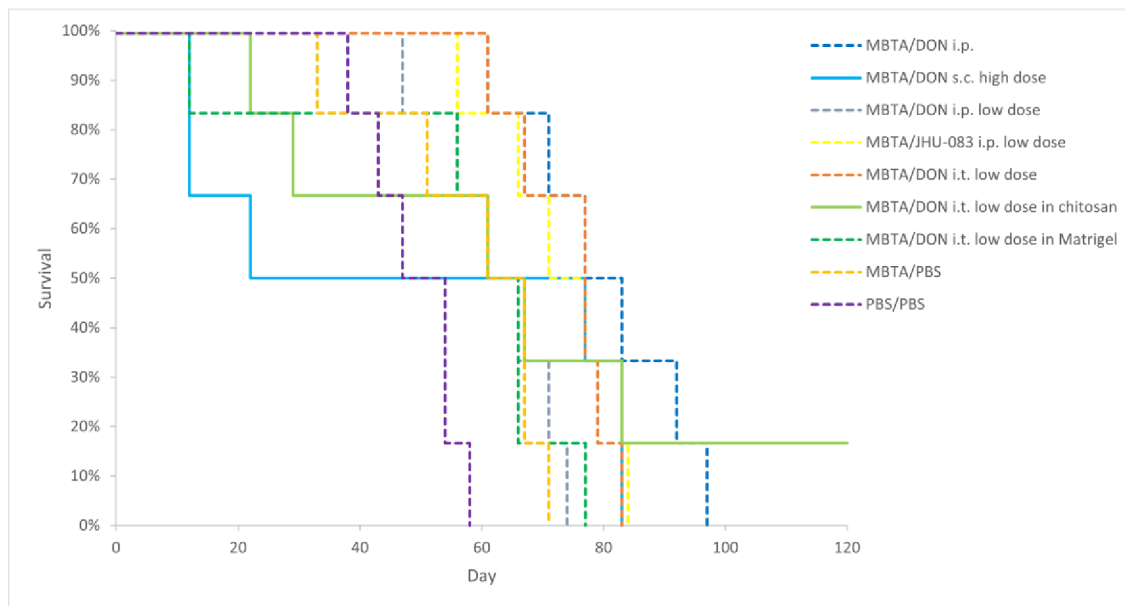


Figure 13: Survival for experiment 2.

Figure 13 depicts a survival graph of the groups in experiment 2. All mice died, except for one in group F which lived past the 120 day observation window. A comparison between DON and JHU-083 with control is shown in figure 14. Figure 15 describes the

differences between intraperitoneal application and different types of intratumoral application. Figure 16 compares low and high dose DON given i.p., high dose DON given s.c. and control.

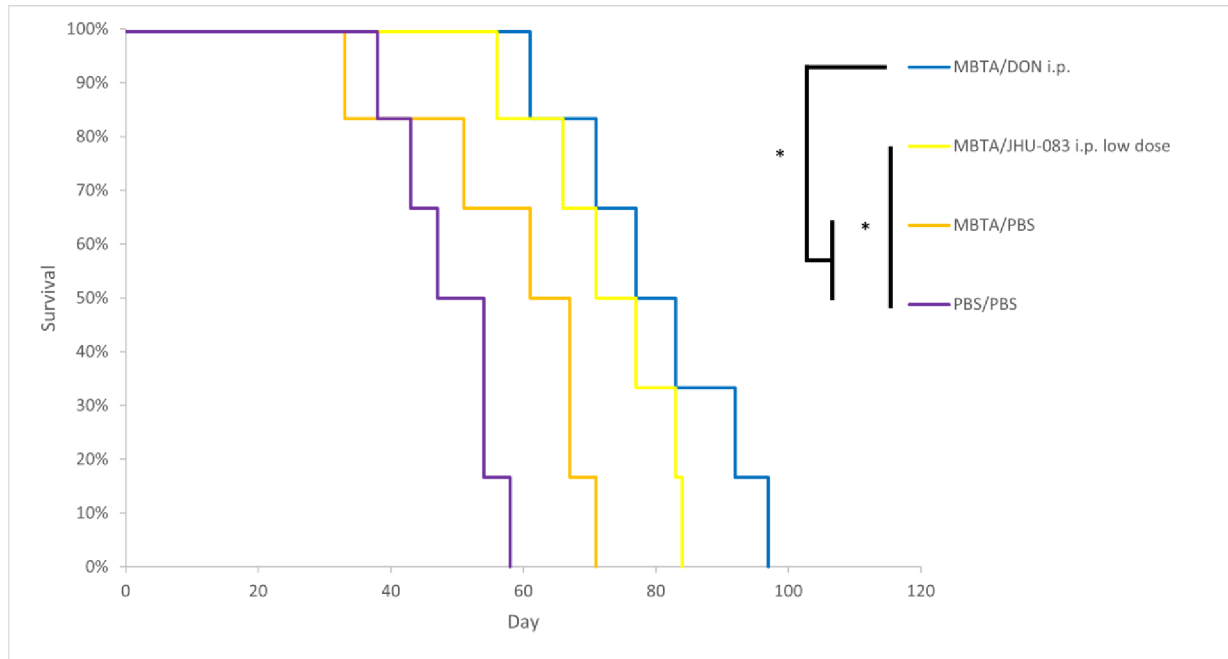


Figure 14: Survival comparison between DON and JHU-083 for experiment 2. * $p \leq 0.05$

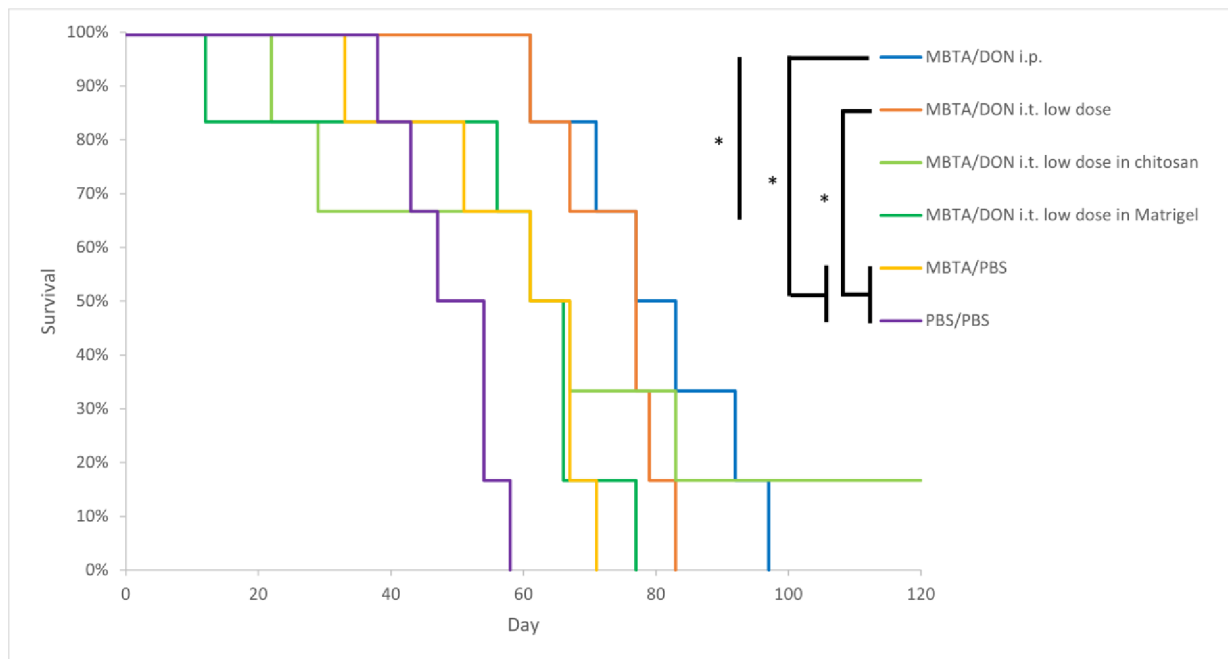


Figure 15: Survival comparison between intraperitoneal application and different types of intratumoral application for experiment 2. * $p \leq 0.05$

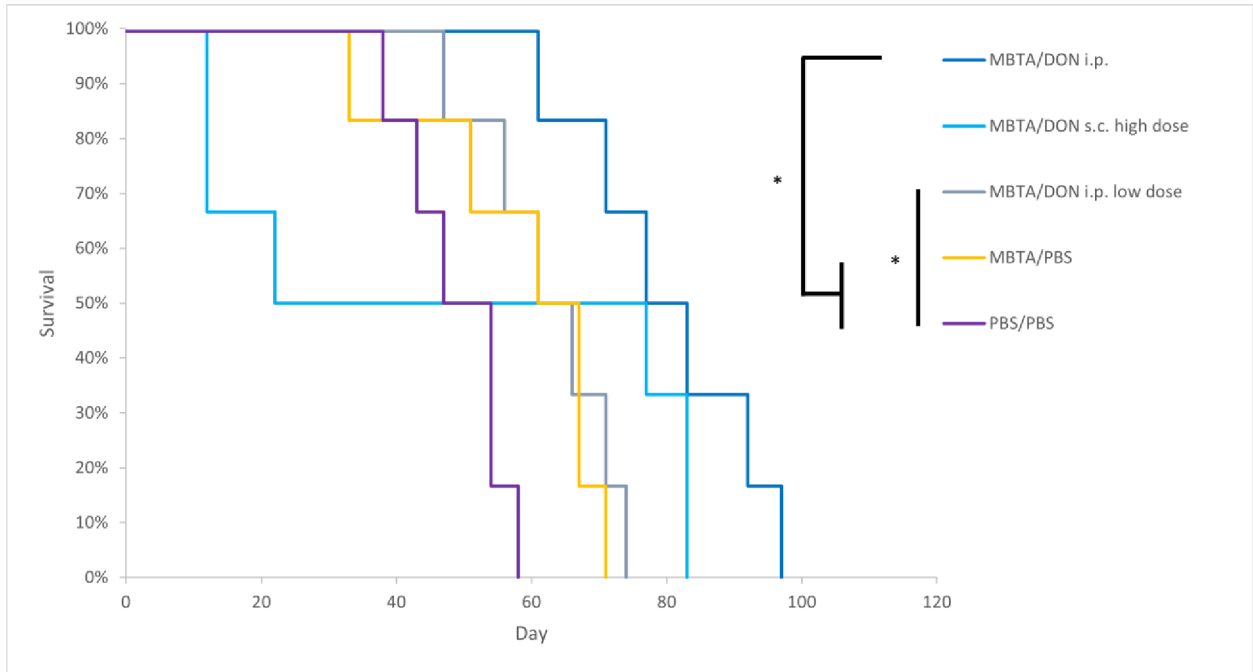


Figure 16: Survival comparison of two dosages of DON given via intraperitoneal application and high dose subcutaneous application for experiment 2. * $p \leq 0.05$

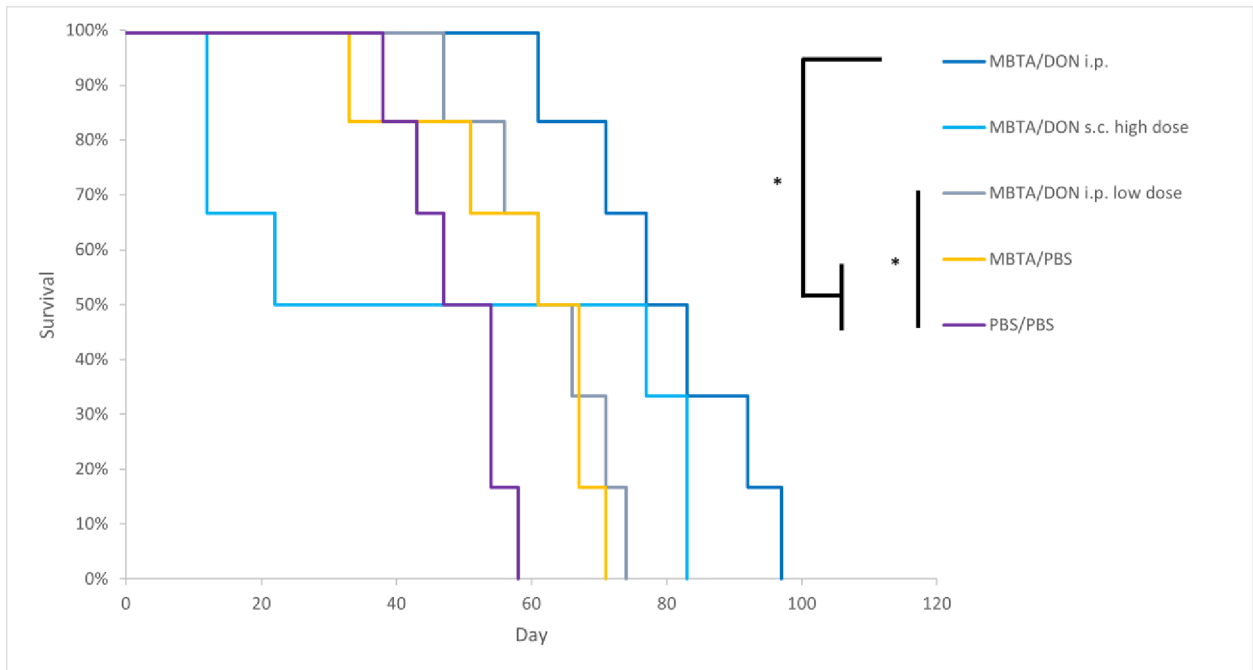


Figure 16: Survival comparison of two dosages of DON given via intraperitoneal application and high dose subcutaneous application for experiment 2. * $p \leq 0.05$

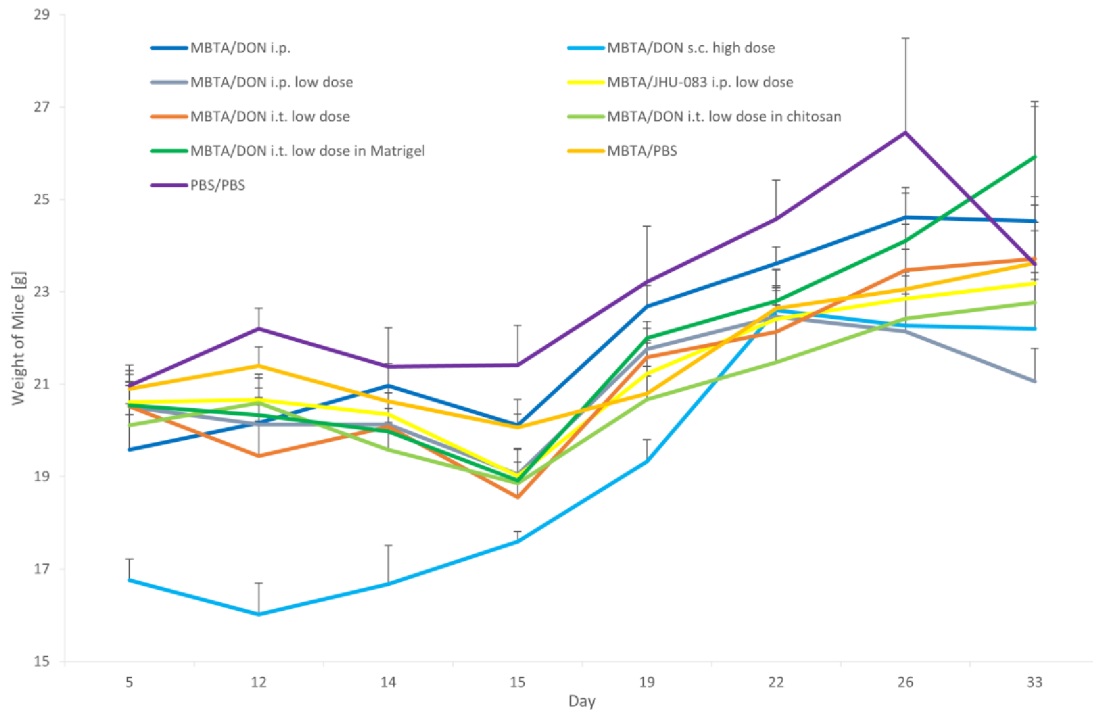


Figure 17: Weight change in experiment 2.

As a measure of side effects, mice weight as well as water and food consumption were evaluated between all groups. Figure 17 shows the mean weight of all groups over the course of the experiment. The general trend is for the weight to fluctuate around 20 g until an increase is observed in all groups except B after the 2-week mark. Again, the area under the curve was calculated. The lowest mean weight was observed in group B which differed significantly ($p \leq 0.05$) from groups A, E, and D (Figure 18). There was no statistically significant difference between group B and control (Figure 19).

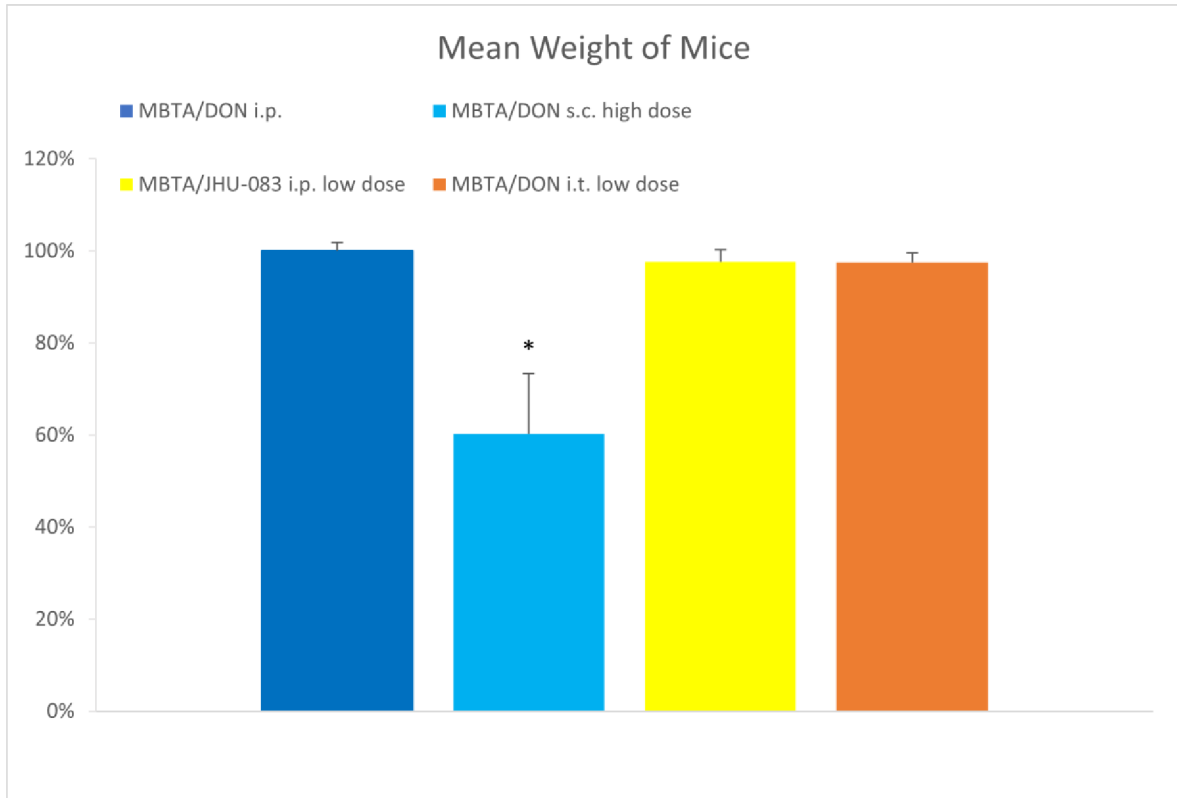


Figure 48: AUC calculation of weight change in groups A, B, D, and E in experiment 2. * $p \leq 0.05$

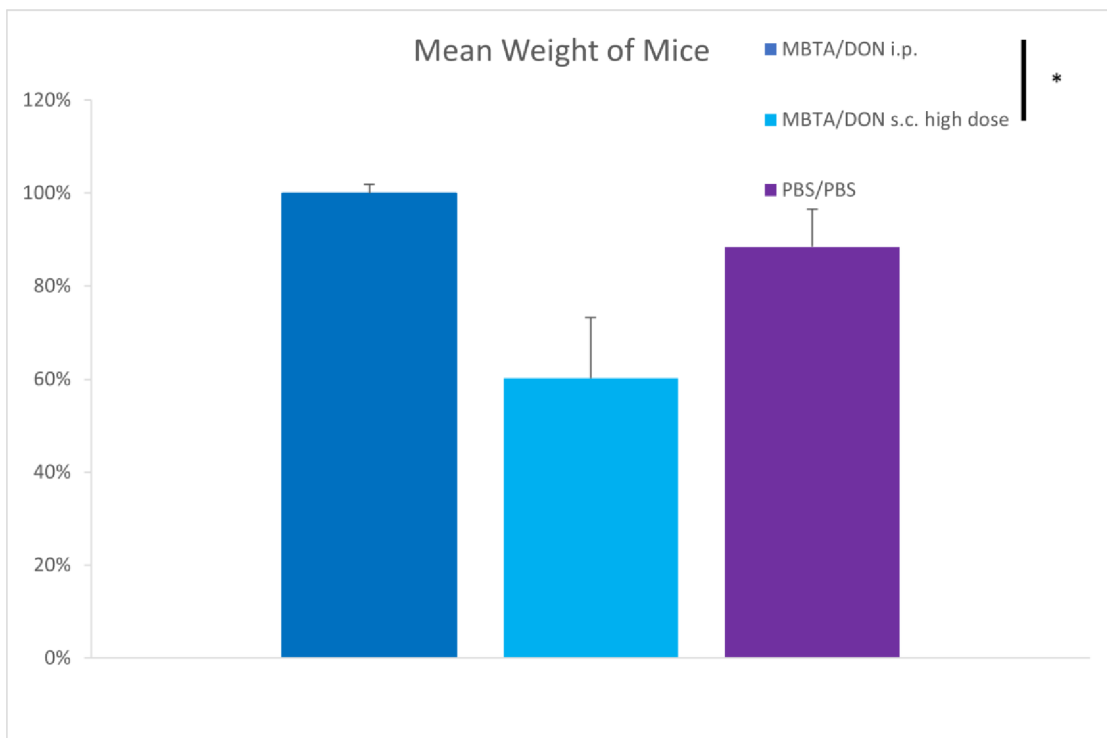


Figure 19: AUC calculation of weight change in groups A, B, and I in experiment 2. * $p \leq 0.05$

4.2.3. Food Consumption

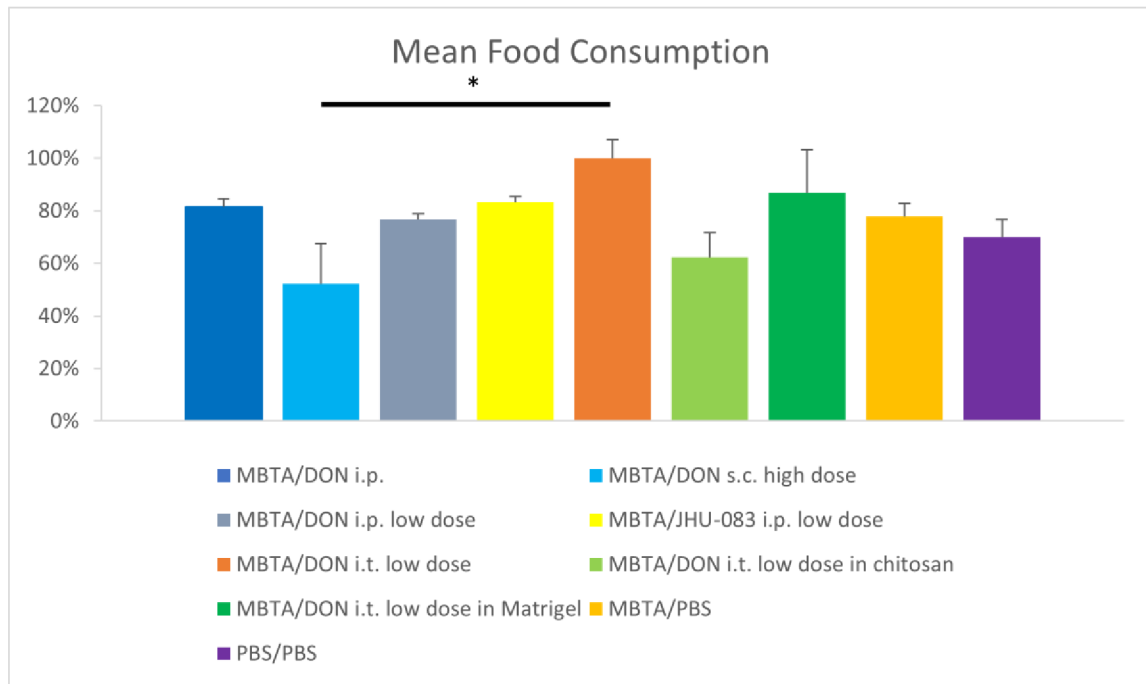


Figure 20: AUC calculation of food consumption in experiment 2. * $p \leq 0.05$

Groups B and E showed a significant difference in the amount of food consumed, with no statistically significant difference to control (Figure 19). Differences between other groups were not statistically significant (Figure 20).

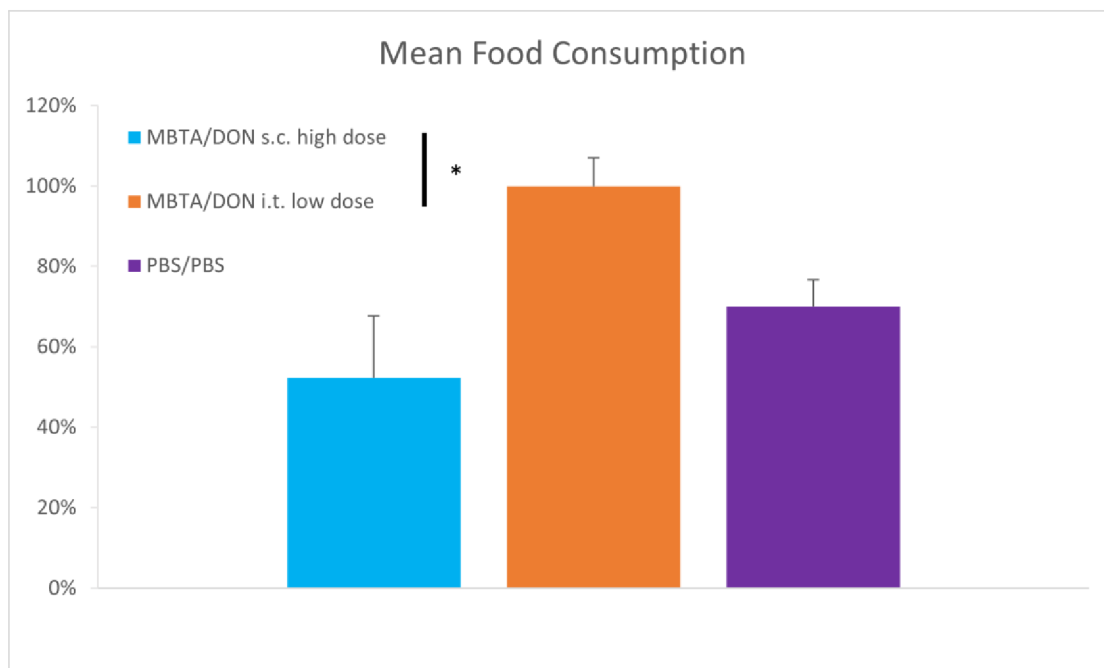


Figure 21: AUC comparison of food consumption of groups B, E, and I in experiment 2. * $p \leq 0.05$

4.2.4. Water Consumption

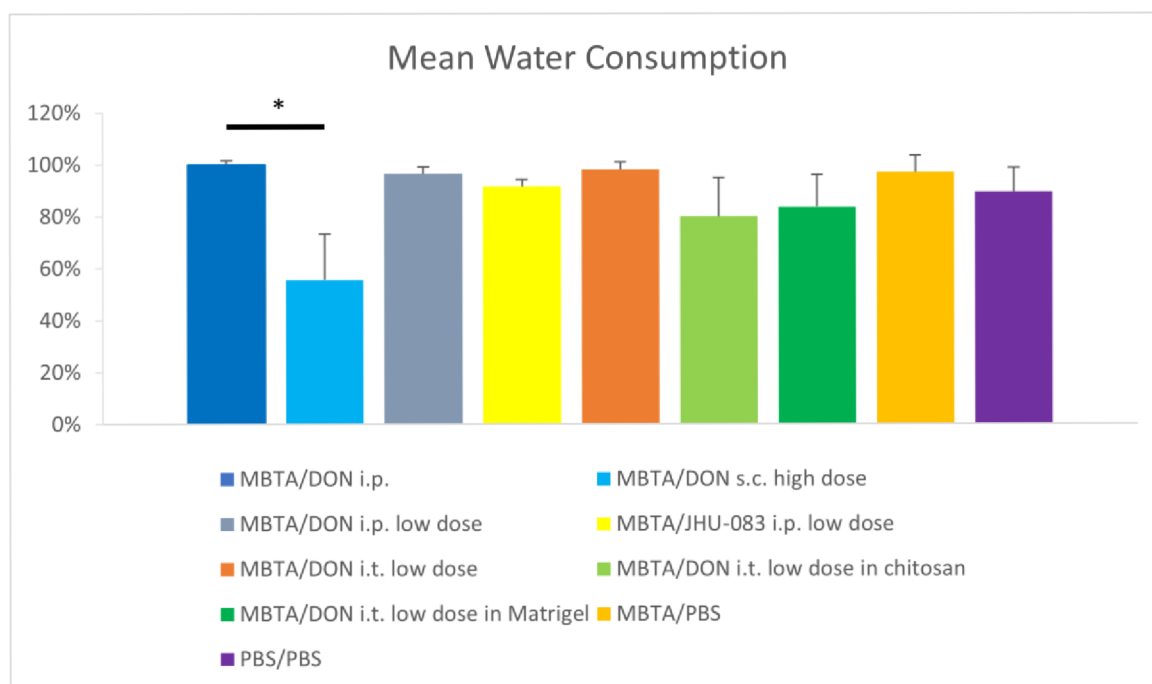


Figure 22: AUC comparison of water consumption for experiment 2. * $p \leq 0.05$

Even though there was only a statistically significant difference between groups A and B, group B consumed the least water out of all the groups (Figure 22). There were no other statistically significant differences between groups.

4.3. Experiment III

4.3.1. Mean Tumor Growth

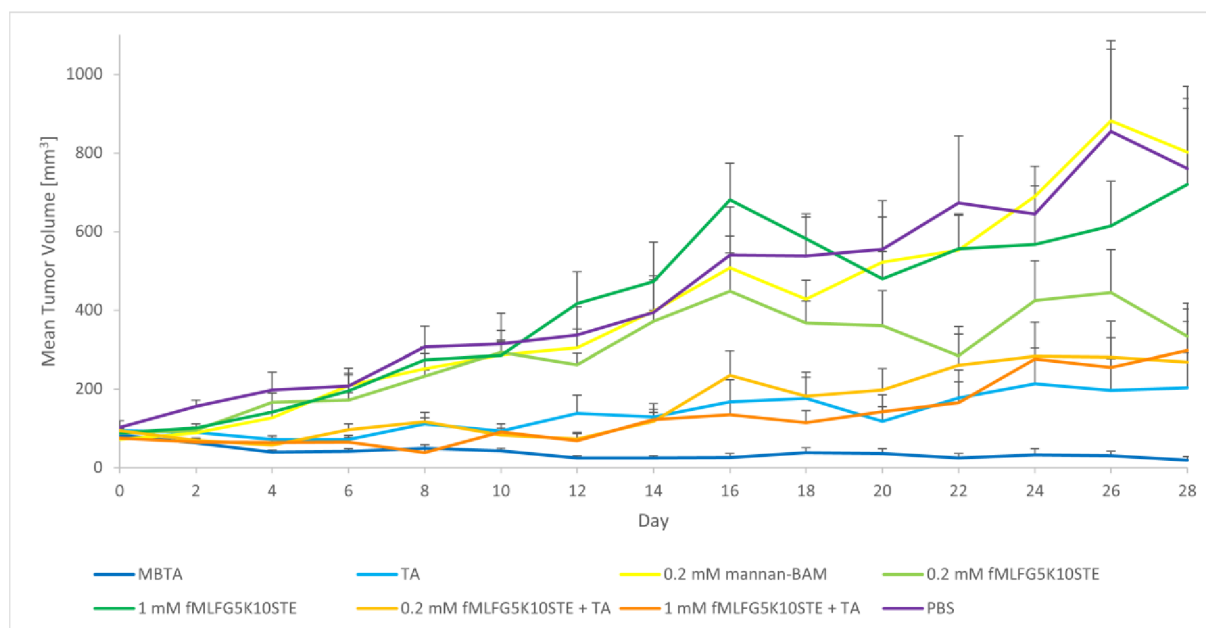


Figure 23: Tumor growth for experiment 3.

The third experiment investigated the replacement of mannan-BAM by fMLFG5K10STE. There was only one tumor as opposed to the other two experiments. Tumor growth over time for the respective groups is depicted in figure 23. AUC was calculated and the fMLF groups did not significantly outperform the MBTA control arm (Figure 24).

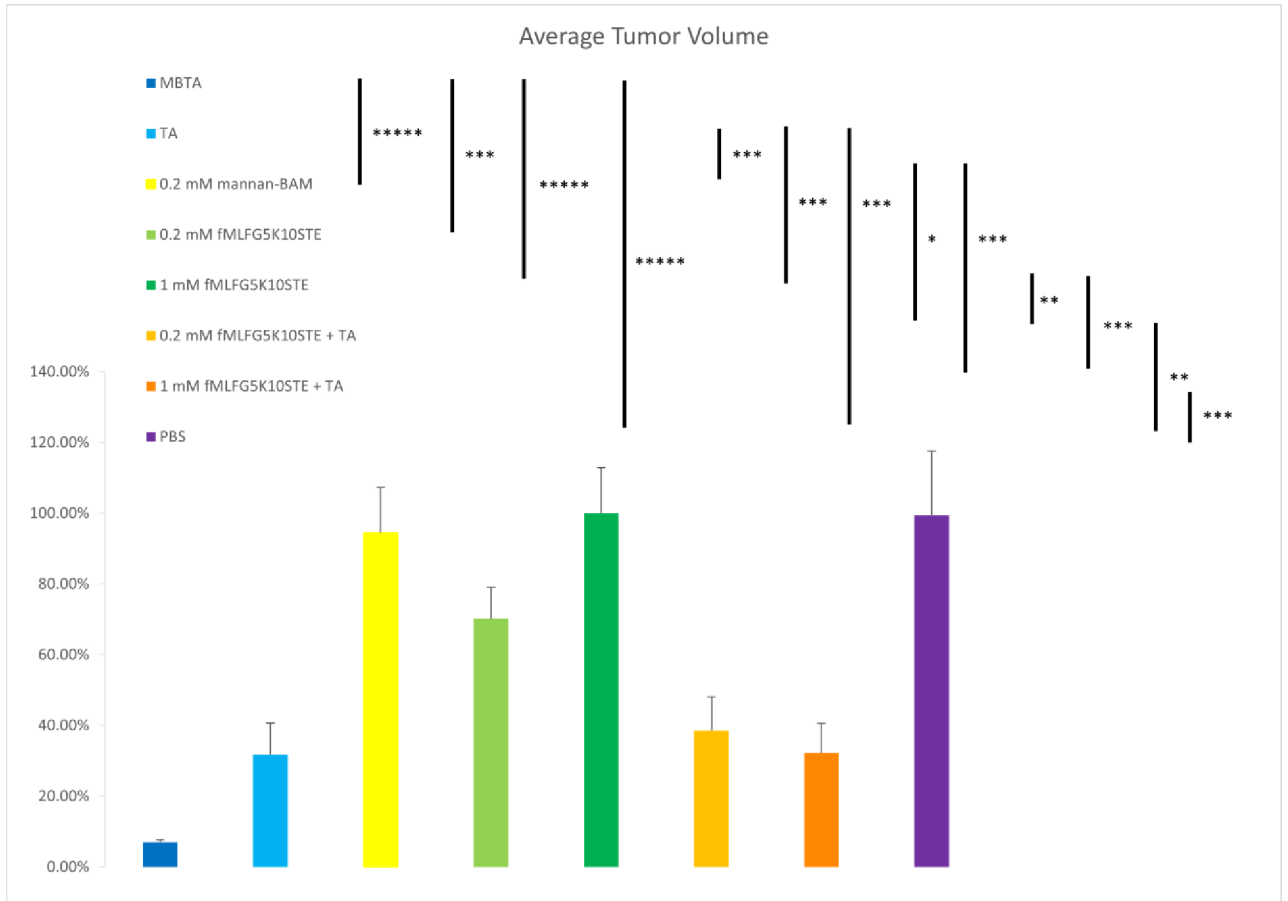


Figure 24: AUC comparison of tumor volume across groups for experiment 3. * $p \leq 0.05$, ** $p \leq 0.01$, *** $p \leq 0.005$, ***** $p \leq 0.0005$

4.3.2. Survival

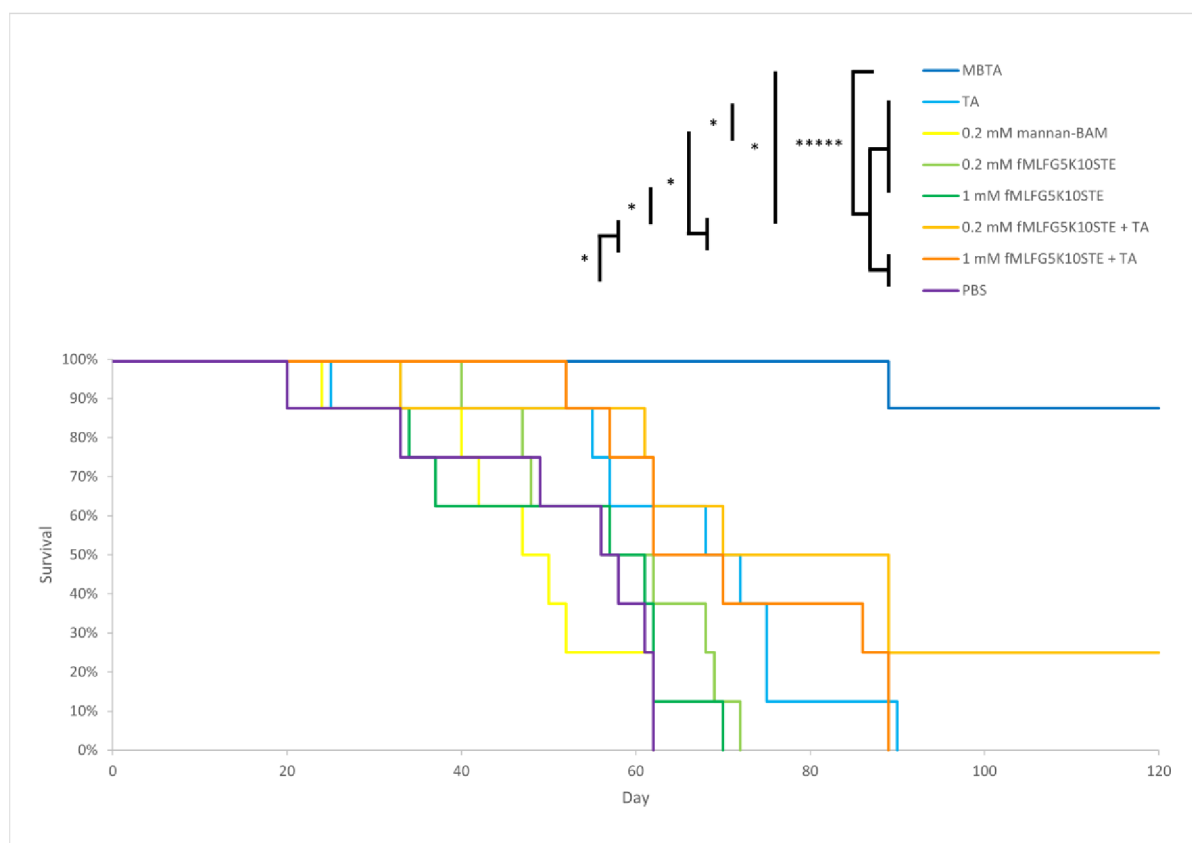


Figure 25: Survival analysis for experiment 3. * $p \leq 0.05$, **** $p \leq 0.0005$

The first group vastly outperformed all other treatment arms (Figure 25). Seven out of 8 mice in the MBTA group survived the entire 120 day monitoring period. One died on day 89. In group F, there were two survivors.

5. Discussion

The Panc02 cell line is aggressive in nature (Partecke et al., 2011; Torres et al., 2013), dense stroma hinder the infiltration of immune cells (Caisová et al., 2018). MBTA is combined with DON in order to achieve a synergistic effect. Immunotherapy by itself is only effective to a certain degree and is often insufficient in curing more complex cases of cancer (Lencová, 2020). Another limitation is the issue of direct application into the tumor, especially when dealing with a tumor that has metastasized, which needs to be accounted for given the high prevalence of metastases in human pancreatic adenocarcinoma (Vareedayah et al., 2018). We found that the presence of another untreated tumor caused “a negative impact on the curability of the treated tumor in the two-tumor model” (Lencová, 2020).

Various synergistic approaches have already been explored, to differing degrees of success. MBTA has been combined with radiotherapy with mildly positive results (Lencová, 2020; Uher et al. 2021). Our colleagues focused primarily on the possibilities of combining immunotherapy with chemotherapy. ONC201, ONC212 (Oncoceutics), doxo-HPMA (Skaličková, 2020), YM155, a survivin inhibitor (Venhauerová, 2020) and Vinblastine and Acriflavine (Lencová, 2020) all delivered sub-par results. The combination of MBTA with DON was the only one that seemed promising (Danielová, 2022; Frejlichová, 2020; Skaličková, 2020).

The Panc02 cell line is aggressive in nature (Partecke et al., 2011; Torres et al., 2013), dense stroma hinder the infiltration of immune cells (Caisová et al., 2018). MBTA is combined with DON in order to achieve a synergistic effect. Immunotherapy by itself is only effective to a certain degree and is often insufficient in curing more complex cases of cancer (Lencová, 2020). Another limitation is the issue of direct application into the tumor, especially when dealing with a tumor that has metastasized, which needs to be accounted for given the high prevalence of metastases in human pancreatic adenocarcinoma (Vareedayah et al., 2018). We

found that the presence of another untreated tumor caused “a negative impact on the curability of the treated tumor in the two-tumor model” (Lencová, 2020). Therefore, it was necessary to try to strengthen the effect of MBTA immunotherapy or to combine it with another therapeutic approach.

Failing to increase therapeutic effect, several combinations of therapeutic approaches were tested to differing degrees of success. MBTA has been combined with radiotherapy with mildly positive results (Lencová, 2020; Uher et al. 2021). The combination with resection is currently being tested (Lencová, oral communication). Our colleagues also focused on the possibilities of combining immunotherapy with chemotherapy. ONC201, ONC212 (Oncoceutics), doxo-HPMA (Skaličková, 2020), YM155, a survivin inhibitor (Venhauerová, 2020), and Vinblastine and Acriflavine (Lencová, 2020) all delivered sub-par results. The combination of MBTA with DON was the only one that seemed promising (Danielová, 2022; Frejlichová, 2020; Skaličková, 2020).

The efficacy of chemotherapy generally increases with higher doses, but so do the side effects (Prieto-Callejero et al., 2020). The first experiment was conducted in order to establish a dose-response relationship and to determine a maximum dose past which the side effects outweigh the therapeutic benefits. It was apparent past a certain threshold, DON’s side effects pose more of a threat to the animal than the cancer itself. The side effects from DON killed the mice in the higher dosed groups and could not fully cure the mice in the lowest dose group. The management of two sizable tumors appears to present a significant challenge, even when employing a combination therapy involving MBTA and DON. two-week mark.

We compared different ways of administering DON. The second experiment also reinforced the finding that direct application of MBTA causes significant reductions in size of the target tumors, as is evident when comparing tumor growth on the right and left flank. Because the dosage distributes systemically when given subcutaneously, there is also an

observed reduction in tumor growth on the left side in the group receiving high dose DON subcutaneously. The use of different carrier media for intratumoral application had some effect on reducing tumor size but did not improve survival.(Earhart et al., 1990). Prodrugs to DON that are to be converted once inside the tumor have been investigated (Rais et al., 2016, 2019). Direct application of therapeutics into the tumor is a promising approach to reduce systemic toxicity in humans (Melero et al., 2021). Our research showed that in mice, intraperitoneal application works best (Danielová, 2022).

MBTA is a promising therapeutic approach (Caisová et al., 2018; Uher et al., 2019, 2021) and has delivered promising results in mice. It seems to induce minimal side effects (Lencová, oral communication). In order to find a mixture compliant with GMP standards, we investigated fMLF as a potential alternative for mannan-BAM. Unfortunately, it did not prove to be a suitable replacement. We suspect that fMLF reacted with poly(I:C), forming a precipitate and rendering it ineffective. If repeated, the experiment can be improved upon by making subtle changes to the molecule. The original MBTA treatment greatly outperformed the others and cured seven out of eight mice.

MBTA is a promising therapeutic approach and has delivered promising results in mice (Caisová et al., 2018; Uher et al., 2019, 2021). It seems to induce minimal side effects (Lencová, oral communication). In order to find a mixture compliant with GMP standards, we investigated fMLF as a potential alternative for mannan-BAM. Unfortunately, it did not prove to be a suitable replacement. We suspect that fMLF reacted with poly(I:C), forming a precipitate and rendering it ineffective. If repeated, the experiment can be improved upon by making subtle changes to the molecule. The original MBTA treatment greatly outperformed the others and cured seven out of eight mice.

6. Conclusion

- There is a point in dosing DON past which the side effects far outweigh its therapeutic potential, killing mice faster than the cancer would.
- For MBTA, intratumoral application works best.
- It remains unclear whether fMLFG5K10STE is suitable for replacing mannan-BAM in the MBTA mixture. Further research is needed to rule out possible interactions.

7. References

- Ahonen, C. L., Doxsee, C. L., McGurran, S. M., Riter, T. R., Wade, W. F., Barth, R. J., Vasilakos, J. P., Noelle, R. J., & Kedl, R. M. (2004). Combined TLR and CD40 Triggering Induces Potent CD8+ T Cell Expansion with Variable Dependence on Type I IFN. *The Journal of Experimental Medicine*, *199*(6), 775.
<https://doi.org/10.1084/JEM.20031591>
- Alberts, B., Johnson, A., Lewis, J., Raff, M., Roberts, K., & Walter, P. (2002). *Innate Immunity*. <https://www.ncbi.nlm.nih.gov/books/NBK26846/>
- Caisová, V., Uher, O., Nedbalová, P., Jochmanová, I., Kvardová, K., Masáková, K., Krejčová, G., Paďouková, L., Chmelař, J., Kopecký, J., & Ženka, J. (2018). Effective cancer immunotherapy based on combination of TLR agonists with stimulation of phagocytosis. *International Immunopharmacology*, *59*, 86–96.
<https://doi.org/10.1016/J.INTIMP.2018.03.038>
- Chaplin, D. D. (2010). Overview of the Immune Response. *The Journal of Allergy and Clinical Immunology*, *125*(2 Suppl 2), S3.
<https://doi.org/10.1016/J.JACI.2009.12.980>
- Conlon, K. C., Miljkovic, M. D., & Waldmann, T. A. (2019). Cytokines in the Treatment of Cancer. *Journal of Interferon & Cytokine Research*, *39*(1), 6.
<https://doi.org/10.1089/JIR.2018.0019>
- Danielová, K. (2022). *Studium imunitní paměti při imunoterapii pankreatického adenokarcinomu*. [Diploma thesis]. University of South Bohemia.
- DeVita, V. T., & Chu, E. (2008). A History of Cancer Chemotherapy. *Cancer Research*, *68*(21), 8643–8653. <https://doi.org/10.1158/0008-5472.CAN-07-6611>
- Earhart, R. H., Amato, D. J., Yuang-Chi Chang, A., Borden, E. C., Shiraki, M., Dowd, M. E., Comis, R. L., Davis, T. E., & Smith, T. J. (1990). Phase II trial of 6-diazo-5-

- oxo-L-norleucine versus aclacinomycin-A in advanced sarcomas and mesotheliomas. *Investigational New Drugs*, 8(1), 113–119.
<https://doi.org/10.1007/BF00216936>
- Eiz-Vesper, B., & Schmetzer, H. M. (2020). Antigen-Presenting Cells: Potential of Proven und New Players in Immune Therapies. *Transfusion Medicine and Hemotherapy*, 47(6), 429. <https://doi.org/10.1159/000512729>
- Fouad, Y. A., & Aanei, C. (2017). Revisiting the hallmarks of cancer. *American Journal of Cancer Research*, 7(5), 1016. [/pmc/articles/PMC5446472/](https://pubmed.ncbi.nlm.nih.gov/35446472/)
- Frejlichová, A. (2020). *Adenosin a nádorová imunoterapie* [Diploma Thesis]. University of South Bohemia.
- Guha, M. (2012). Anticancer TLR agonists on the ropes. *Nature Reviews Drug Discovery*, 11(7), 503–505. <https://doi.org/10.1038/NRD3775>
- Gutterman, J. U. (1994). Cytokine therapeutics: lessons from interferon alpha. *Proceedings of the National Academy of Sciences of the United States of America*, 91(4), 1198–1205. <https://doi.org/10.1073/PNAS.91.4.1198>
- Hanahan, D. (2022). Hallmarks of Cancer: New Dimensions. *Cancer Discovery*, 12(1), 31–46. <https://doi.org/10.1158/2159-8290.CD-21-1059>
- Hanahan, D., & Weinberg, R. A. (2000). The Hallmarks of Cancer. *Cell*, 100(1), 57–70. [https://doi.org/10.1016/S0092-8674\(00\)81683-9](https://doi.org/10.1016/S0092-8674(00)81683-9)
- Hanahan, D., & Weinberg, R. A. (2011). Hallmarks of cancer: The next generation. *Cell*, 144(5), 646–674.
<https://doi.org/10.1016/J.CELL.2011.02.013/ATTACHMENT/3F528E16-8B3C-4D8D-8DE5-43E0C98D8475/MMC1.PDF>
- Hassan, S. B., Sorensen, J. F., Olsen, B. N., & Pedersen, A. E. (2014). Anti-CD40-mediated cancer immunotherapy: an update of recent and ongoing clinical trials.

[Http://Dx.Doi.Org/10.3109/08923973.2014.890626](http://dx.doi.org/10.3109/08923973.2014.890626), 36(2), 96–104.

<https://doi.org/10.3109/08923973.2014.890626>

He, H. Q., & Ye, R. D. (2017). The Formyl Peptide Receptors: Diversity of Ligands and Mechanism for Recognition. *Molecules : A Journal of Synthetic Chemistry and Natural Product Chemistry*, 22(3). <https://doi.org/10.3390/MOLECULES22030455>

Heiden, M. G. V., Cantley, L. C., & Thompson, C. B. (2009). Understanding the Warburg Effect: The Metabolic Requirements of Cell Proliferation. *Science (New York, N.Y.)*, 324(5930), 1029. <https://doi.org/10.1126/SCIENCE.1160809>

Hemmi, H., Kaisho, T., Takeuchi, O., Sato, S., Sanjo, H., Hoshino, K., Horiuchi, T., Tomizawa, H., Takeda, K., & Akira, S. (2002). Small anti-viral compounds activate immune cells via the TLR7 MyD88-dependent signaling pathway. *Nature Immunology*, 3(2), 196–200. <https://doi.org/10.1038/NI758>

Hessle, C., Andersson, B., & Wold, A. E. (2000). Gram-positive bacteria are potent inducers of monocytic interleukin-12 (IL-12) while gram-negative bacteria preferentially stimulate IL-10 production. *Infection and Immunity*, 68(6), 3581–3586. <https://doi.org/10.1128/IAI.68.6.3581-3586.2000>

Janeway, C. A., & Medzhitov, R. (2002). Innate immune recognition. *Annual Review of Immunology*, 20, 197–216.

<https://doi.org/10.1146/ANNUREV.IMMUNOL.20.083001.084359>

Janotová, T., Jalovecká, M., Auerová, M., Švecová, I., Bruzlová, P., Maierová, V., Kumžáková, Z., Čunátová, Š., Vlčková, Z., Caisová, V., Rozsypalová, P., Lukáčová, K., Vácová, N., Wachtlová, M., Salát, J., Lieskovská, J., Kopecký, J., & Ženka, J. (2014). The use of anchored agonists of phagocytic receptors for cancer immunotherapy: B16-F10 murine melanoma model. *PloS One*, 9(1).

<https://doi.org/10.1371/JOURNAL.PONE.0085222>

- Johnson, D. B., Nebhan, C. A., Moslehi, J. J., & Balko, J. M. (2022). Immune-checkpoint inhibitors: long-term implications of toxicity. *Nature Reviews Clinical Oncology* 2022 19:4, 19(4), 254–267. <https://doi.org/10.1038/s41571-022-00600-w>
- Jurk, M., Heil, F., Vollmer, J., Schetter, C., Krieg, A. M., Wagner, H., Lipford, G., & Bauer, S. (2002). Human TLR7 or TLR8 independently confer responsiveness to the antiviral compound R-848. *Nature Immunology*, 3(6), 499. <https://doi.org/10.1038/NI0602-499>
- Kato, K., Itoh, C., Yasukouchi, T., & Nagamune, T. (2004). Rapid protein anchoring into the membranes of Mammalian cells using oleyl chain and poly(ethylene glycol) derivatives. *Biotechnology Progress*, 20(3), 897–904. <https://doi.org/10.1021/BP0342093>
- Kaufmann, S. H. E. (2008). Paul Ehrlich: founder of chemotherapy. *Nature Reviews Drug Discovery* 2008 7:5, 7(5), 373–373. <https://doi.org/10.1038/nrd2582>
- Kawasaki, T., & Kawai, T. (2014). Toll-like receptor signaling pathways. *Frontiers in Immunology*, 5(SEP), 461. <https://doi.org/10.3389/FIMMU.2014.00461/BIBTEX>
- Lemberg, K. M., Vornov, J. J., Rais, R., & Slusher, B. S. (2018). We’re Not “DON” Yet: Optimal Dosing and Prodrug Delivery of 6-Diazo-5-oxo-L-norleucine. *Molecular Cancer Therapeutics*, 17(9), 1824–1832. <https://doi.org/10.1158/1535-7163.MCT-17-1148>
- Lencová, R. (2020). *Nádorová imunoterapie pankreatického adenokarcinomu založená na synergii agonistů TLR a ligandů stimulujících fagocytózu a její protimetastázový účinek* [Diploma Thesis]. University of South Bohemia.
- Lipke, P. N., & Ovalle, R. (1998). Cell wall architecture in yeast: new structure and new challenges. *Journal of Bacteriology*, 180(15), 3735–3740. <https://doi.org/10.1128/JB.180.15.3735-3740.1998>

- Marshall, J. S., Warrington, R., Watson, W., & Kim, H. L. (2018). An introduction to immunology and immunopathology. *Allergy, Asthma and Clinical Immunology*, 14(2), 1–10. <https://doi.org/10.1186/S13223-018-0278-1/TABLES/4>
- Medina, R., Wang, H., Caisová, V., Cui, J., Indig, I. H., Uher, O., Ye, J., Nwankwo, A., Sanchez, V., Wu, T., Nduom, E., Heiss, J., Gilbert, M. R., Terabe, M., Ho, W., Zenka, J., Pacak, K., & Zhuang, Z. (2020). Induction of Immune Response Against Metastatic Tumors via Vaccination of Mannan-BAM, TLR Ligands and Anti-CD40 Antibody (MBTA). *Advanced Therapeutics*, 3(9). <https://doi.org/10.1002/ADTP.202000044>
- Melero, I., Castanon, E., Alvarez, M., Champiat, S., & Marabelle, A. (2021). Intratumoural administration and tumour tissue targeting of cancer immunotherapies. *Nature Reviews Clinical Oncology* 2021 18:9, 18(9), 558–576. <https://doi.org/10.1038/s41571-021-00507-y>
- Napolitani, G., Rinaldi, A., Bertonni, F., Sallusto, F., & Lanzavecchia, A. (2005). Selected Toll-like receptor agonist combinations synergistically trigger a T helper type 1-polarizing program in dendritic cells. *Nature Immunology*, 6(8), 769–776. <https://doi.org/10.1038/NI1223>
- Oiseth, S. J., & Aziz, M. S. (2017). Cancer immunotherapy: a brief review of the history, possibilities, and challenges ahead. *Journal of Cancer Metastasis and Treatment*, 3(10), 250–261. <https://doi.org/10.20517/2394-4722.2017.41>
- Panaro, M. A., & Mitolo, V. (1999). Cellular responses to FMLP challenging: a mini-review. *Immunopharmacology and Immunotoxicology*, 21(3), 397–419. <https://doi.org/10.3109/08923979909007117>
- Partecke, L. I., Sandler, M., Kaeding, A., Weiss, F. U., Mayerle, J., Dummer, A., Nguyen, T. D., Albers, N., Speerforck, S., Lerch, M. M., Heidecke, C. D., Von

- Bernstorff, W., & Stier, A. (2011). A syngeneic orthotopic murine model of pancreatic adenocarcinoma in the C57/BL6 mouse using the Panc02 and 6606PDA cell lines. *European Surgical Research. Europäische Chirurgische Forschung. Recherches Chirurgicales Europeennes*, 47(2), 98–107.
<https://doi.org/10.1159/000329413>
- Prieto-Callejero, B., Rivera, F., Fagundo-Rivera, J., Romero, A., Romero-Martín, M., Gómez-Salgado, J., & Ruiz-Frutos, C. (2020). Relationship between chemotherapy-induced adverse reactions and health-related quality of life in patients with breast cancer. *Medicine*, 99(33), e21695. <https://doi.org/10.1097/MD.00000000000021695>
- Rais, R., Alt, J., Dash, R., Tenora, L., Majer, P., & Slusher, B. S. (2019). Tumor targeted delivery of glutamine antagonist: Use of CES1^{-/-} mice. *Cancer Research*, 79(13), 3620–3620. <https://doi.org/10.1158/1538-7445.AM2019-3620>
- Rais, R., Jančařík, A., Tenora, L., Nedelcovych, M., Alt, J., Englert, J., Rojas, C., Le, A., Elgogary, A., Tan, J., Monincová, L., Pate, K., Adams, R., Ferraris, D., Powell, J., Majer, P., & Slusher, B. S. (2016). Discovery of 6-Diazo-5-oxo-1-norleucine (DON) Prodrugs with Enhanced CSF Delivery in Monkeys: A Potential Treatment for Glioblastoma. *Journal of Medicinal Chemistry*, 59(18), 8621–8633.
<https://doi.org/10.1021/ACS.JMEDCHEM.6B01069>
- Reis, E. S., Mastellos, D. C., Hajishengallis, G., & Lambris, J. D. (2019). New insights into the immune functions of complement. *Nature Reviews Immunology* 2019 19:8, 19(8), 503–516. <https://doi.org/10.1038/s41577-019-0168-x>
- Singh, S., Kumar, N., Dwiwedi, P., Charan, J., Kaur, R., Sidhu, P., & Chugh, V. (2018). Monoclonal Antibodies: A Review. *Current Clinical Pharmacology*, 13(2), 651–654. <https://doi.org/10.2174/1574884712666170809124728>

- Skaličková, M. (2020). *Imunoterapie metastazujícího pankreatického adenokarcinomu řešená na dvounádorovém modelu*. [Diploma thesis]. University of South Bohemia.
- Sporn, M. B., & Todaro, G. J. (1980). Autocrine Secretion and Malignant Transformation of Cells. *New England Journal of Medicine*, 303(15), 878–880. <https://doi.org/10.1056/NEJM198010093031511>
- Sterner, R. C., & Sterner, R. M. (2021). CAR-T cell therapy: current limitations and potential strategies. *Blood Cancer Journal* 2021 11:4, 11(4), 1–11. <https://doi.org/10.1038/s41408-021-00459-7>
- Strebhardt, K., & Ullrich, A. (2008). Paul Ehrlich's magic bullet concept: 100 years of progress. *Nature Reviews Cancer* 2008 8:6, 8(6), 473–480. <https://doi.org/10.1038/nrc2394>
- Sung, H., Ferlay, J., Siegel, R. L., Laversanne, M., Soerjomataram, I., Jemal, A., & Bray, F. (2021). Global Cancer Statistics 2020: GLOBOCAN Estimates of Incidence and Mortality Worldwide for 36 Cancers in 185 Countries. *CA: A Cancer Journal for Clinicians*, 71(3), 209–249. <https://doi.org/10.3322/CAAC.21660>
- Świdarska, E., Strycharz, J., Wróblewski, A., Szemraj, J., Drzewoski, J., Śliwińska, A., Świdarska, E., Strycharz, J., Wróblewski, A., Szemraj, J., Drzewoski, J., & Śliwińska, A. (2018). Role of PI3K/AKT Pathway in Insulin-Mediated Glucose Uptake. *Blood Glucose Levels*. <https://doi.org/10.5772/INTECHOPEN.80402>
- Takeuchi, O., Hoshino, K., Kawai, T., Sanjo, H., Takada, H., Ogawa, T., Takeda, K., & Akira, S. (1999). Differential Roles of TLR2 and TLR4 in Recognition of Gram-Negative and Gram-Positive Bacterial Cell Wall Components. *Immunity*, 11(4), 443–451. [https://doi.org/10.1016/S1074-7613\(00\)80119-3](https://doi.org/10.1016/S1074-7613(00)80119-3)
- Talmadge, J. E., Adams, J., Phillips, H., Collins, M., Lenz, B., Schneider, M., Schlick, E., Ruffmann, R., Wiltrout, R. H., & Chirigos, M. A. (1985). Immunomodulatory

Effects in Mice of Polyinosinic-Polycytidylic Acid Complexed with Poly-L-lysine and Carboxymethylcellulose. *Cancer Research*, 45(3), 1058–1065.

<https://experts.nebraska.edu/en/publications/immunomodulatory-effects-in-mice-of-polyinosinic-polycytidylic-ac>

Tenora, L., Alt, J., Dash, R. P., Gadiano, A. J., Novotná, K., Veeravalli, V., Lam, J., Kirkpatrick, Q. R., Lemberg, K. M., Majer, P., Rais, R., & Slusher, B. S. (2019). Tumor-Targeted Delivery of 6-Diazo-5-oxo-1-norleucine (DON) Using Substituted Acetylated Lysine Prodrugs. *Journal of Medicinal Chemistry*, 62(7), 3524–3538.

https://doi.org/10.1021/ACS.JMEDCHEM.8B02009/SUPPL_FILE/JM8B02009_SI_002.CSV

Torres, M. P., Rachagani, S., Soucek, J. J., Mallya, K., Johansson, S. L., & Batra, S. K. (2013). Novel pancreatic cancer cell lines derived from genetically engineered mouse models of spontaneous pancreatic adenocarcinoma: applications in diagnosis and therapy. *PloS One*, 8(11). <https://doi.org/10.1371/JOURNAL.PONE.0080580>

Turner, M. D., Nedjai, B., Hurst, T., & Pennington, D. J. (2014). Cytokines and chemokines: At the crossroads of cell signalling and inflammatory disease. *Biochimica et Biophysica Acta (BBA) - Molecular Cell Research*, 1843(11), 2563–2582. <https://doi.org/10.1016/J.BBAMCR.2014.05.014>

Uher, O., Caisova, V., Hansen, P., Kopecky, J., Chmelar, J., Zhuang, Z., Zenka, J., & Pacak, K. (2019). Coley's immunotherapy revived: innate immunity as a link in priming cancer cells for an attack by adaptive immunity. *Seminars in Oncology*, 46(4–5), 385. <https://doi.org/10.1053/J.SEMINONCOL.2019.10.004>

Uher, O., Caisova, V., Padoukova, L., Kvardova, K., Masakova, K., Lencova, R., Frejlichova, A., Skalickova, M., Venhauerova, A., Chlastakova, A., Hansen, P.,

- Chmelar, J., Kopecky, J., Zhuang, Z., Pacak, K., & Zenka, J. (2021). Mannan-BAM, TLR ligands, and anti-CD40 immunotherapy in established murine pancreatic adenocarcinoma: understanding therapeutic potentials and limitations. *Cancer Immunology, Immunotherapy: CII*, 70(11), 3303–3312.
<https://doi.org/10.1007/S00262-021-02920-9>
- Uribe-Querol, E., & Rosales, C. (2020). Phagocytosis: Our Current Understanding of a Universal Biological Process. *Frontiers in Immunology*, 11, 1066.
<https://doi.org/10.3389/FIMMU.2020.01066/BIBTEX>
- Vareedayah, A. A., Alkaade, S., & Taylor, J. R. (2018). Pancreatic Adenocarcinoma. *Missouri Medicine*, 115(3), 230. <https://doi.org/10.6004/jnccn.2010.0073>
- Venhauerová, A. (2020). *Studium významu a mechanismů zapojení získané imunity při nádorové imunoterapii založené na synergii agonistů TLR a ligandů stimulujících fagocytózu*. University of South Bohemia.
- Waldmannová, E., Caisová, V., Fáberová, J., Sváčková, P., Kovářová, M., Sváčková, D., Kumžáková, Z., Jačková, A., Vácová, N., Nedbalová, P., Horká, M., Kopecký, J., & Ženka, J. (2016). The use of Zymosan A and bacteria anchored to tumor cells for effective cancer immunotherapy: B16-F10 murine melanoma model. *International Immunopharmacology*, 39, 295–306.
<https://doi.org/10.1016/J.INTIMP.2016.08.004>
- Weeks, C. E., & Gibson, S. J. (1994). Induction of interferon and other cytokines by imiquimod and its hydroxylated metabolite R-842 in human blood cells in vitro. *Journal of Interferon Research*, 14(2), 81–85.
<https://doi.org/10.1089/JIR.1994.14.81>
- WHO. (2022, February 3). *Cancer Factsheet*. <https://www.who.int/en/news-room/factsheets/detail/cancer>

- William B. Coley. (1893). The Treatment of Malignant Tumors by Repeated Inoculations of Erysipelas: With a Report of Ten Original Cases. *The American Journal of the Medical Sciences*, 105(6), 487–511.
<https://www.proquest.com/openview/09fb106c24157c028c895edfa8049551/1?pq-origsite=gscholar&cbl=41361>
- Wise, D. R., & Thompson, C. B. (2010). Glutamine Addiction: A New Therapeutic Target in Cancer. *Trends in Biochemical Sciences*, 35(8), 427–433.
<https://doi.org/10.1016/J.TIBS.2010.05.003>
- Zhu, X., Nishimura, F., Sasaki, K., Fujita, M., Dusak, J. E., Eguchi, J., Fellows-Mayle, W., Storkus, W. J., Walker, P. R., Salazar, A. M., & Okada, H. (2007). Toll like receptor-3 ligand poly-ICLC promotes the efficacy of peripheral vaccinations with tumor antigen-derived peptide epitopes in murine CNS tumor models. *Journal of Translational Medicine*, 5(1), 1–15. <https://doi.org/10.1186/1479-5876-5-10/FIGURES/8>